Supporting Information

Easily Accessible Rare-Earth-Containing Phosphonium Room-Temperature Ionic Liquids: EXAFS, Luminescence and Magnetic Properties

Jorge Alvarez-Vicente,[a] Sahra Dandil,[a] Dipanjan Banerjee,[c] H.Q. Nimal Gunaratne,[a] Suzanne Gray,[d] Solveig Felton,[d] Geetha Srinivasan,[a] Anna M. Kaczmarek,[b] Rik Van Deun,[*b] and Peter Nockemann[*a]

Luminescence properties of sample $[P_{4444}]_3[EuCl_6]$

1) Emission spectra

Upon excitation at 394.1 nm (25374 cm^{-1}), in the $^5L_6 \leftarrow {}^7F_0$ transition, the sample shows typical narrow Eu^{3+} emission peaks (Fig. S1). The peaks labelled a-e have been assigned to the corresponding electronic transitions in Table S1.

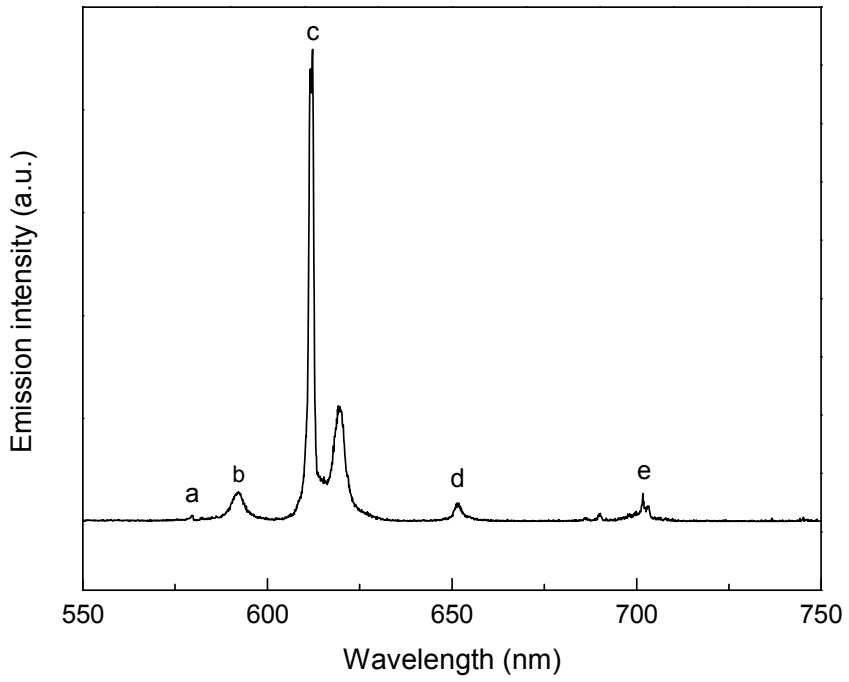

Fig. S1 Emission spectrum of $[P_{4444}]_3[EuCl_6]$, excited at 394.1 nm and corrected for detector sensitivity.

Table S1. Assignment of the 4f-4f transitions in the emission spectrum of $[P_{4444}]_3[EuCl_6]$.

Label	λ (nm)	$\bar{\upsilon}$ (cm^{-1})	Transition
a	579.6	17253	$^5D_0 \rightarrow {}^7F_0$
b	592.3	16883	$^5D_0 \rightarrow {}^7F_1$
c	612.2	16334	$^5D_0 \rightarrow {}^7F_2$
d	651.5	15349	$^5D_0 \rightarrow {}^7F_3$
e	701.6	14253	$^5D_0 \rightarrow {}^7F_4$

The sample was also excited at 347.6 nm (28768 cm^{-1}) giving rise to typical Eu^{3+} peaks as when excited at 394.1 nm, but with slightly lower intensity (Fig. S2).

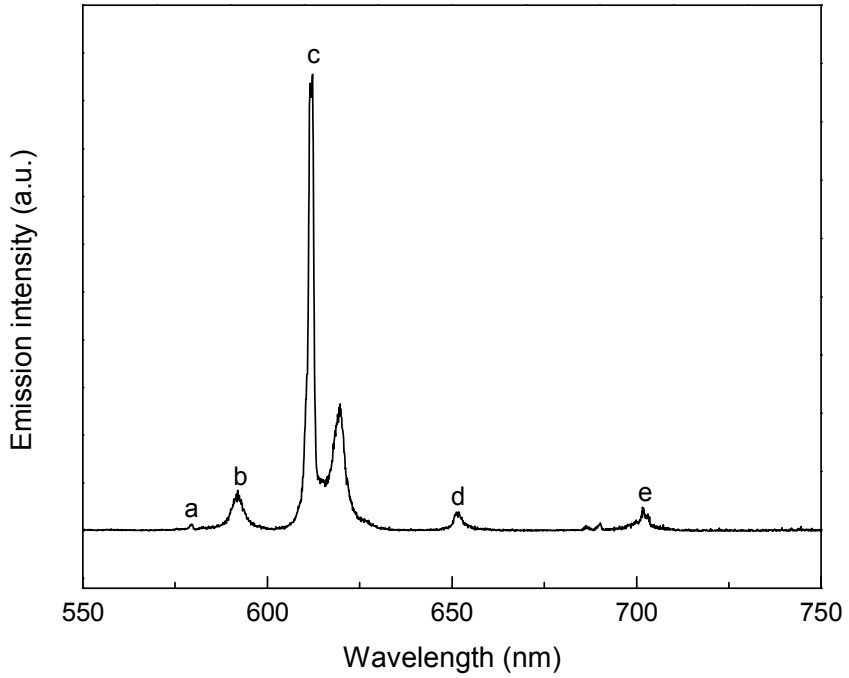

Fig. S2 Emission spectrum of $[P_{4444}]_3[EuCl_6]$, excited at 347.6 nm and corrected for detector sensitivity.

2) Excitation spectrum for $[P_{4444}]_3[EuCl_6]$

Monitoring the emission of the sample at 612.2 nm (16335 cm^{-1}, transition $^5D_0 \rightarrow {}^7F_2$), the excitation wavelength was varied between 250 and 500 nm to record an excitation

spectrum (Fig. 3). In the spectrum a broad band with a maximum at 347.6 nm (28769 cm^{-1}) is visible. All other peaks in the spectrum can be assigned to transitions within the Eu^{3+} ion's 4f shell. The peaks labelled a-i have been assigned to the corresponding transitions in Table S2.

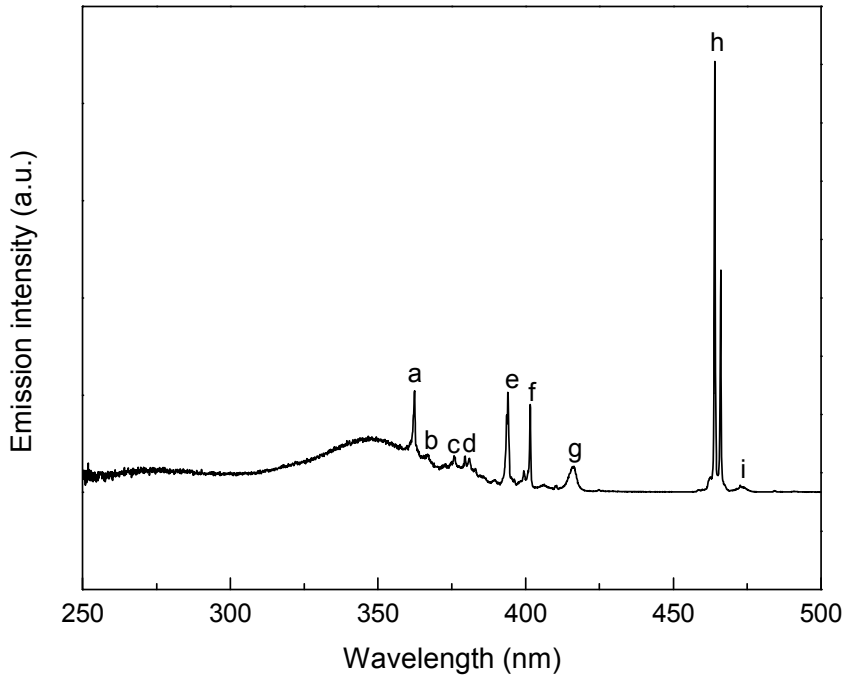

Fig. S3 Excitation spectrum of $[P_{4444}]_3[EuCl_6]$, monitored at 612.2 nm, corrected for detector sensitivity.

Table S2. Assignment of the 4f-4f transitions in the excitation spectrum of $[P_{4444}]_3[EuCl_6]$.

Label	λ (nm)	$\bar{\upsilon}$ (cm^{-1})	Transition
a	362.3	27601	$^5D_4 \leftarrow {}^7F_0$
b	366.8	27263	$^5D_4 \leftarrow {}^7F_1$
c	374.8	26681	$^5G_{6,4} \leftarrow {}^7F_0$
d	379.3	26364	$^5G_{6,5,3} \leftarrow {}^7F_1$
e	394.1	25374	$^5L_6 \leftarrow {}^7F_0$
f	401.5	24907	$^5L_6 \leftarrow {}^7F_1$

g	415.8	24050	$^5D_3 \leftarrow {}^7F_1$
h	464.1	21547	$^5D_2 \leftarrow {}^7F_0$
i	472.7	21155	$^5D_2 \leftarrow {}^7F_1$

3) Luminescence decay time of $[P_{4444}]_3[EuCl_6]$

Upon excitation at 355.0 nm with a pulsed light source, the emission at 612.2 nm shows a mono-exponential decay profile. The luminescence decay profile is given in Fig. S4. The luminescence decay time is calculated as 0.960 ms or 960 µs.

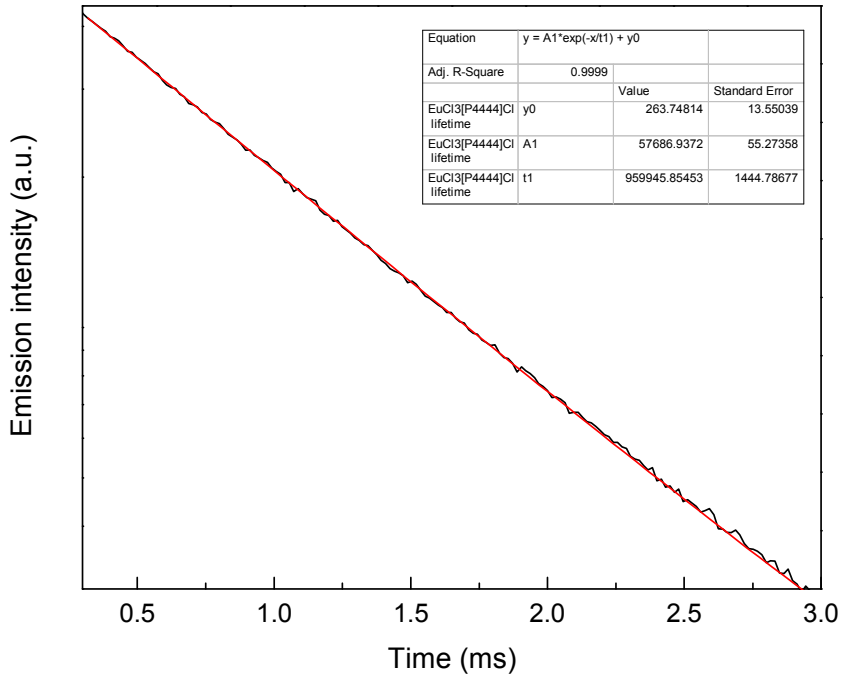

Fig. S4 Luminescence decay profile of $[P_{4444}]_3[EuCl_6]$, upon excitation at 355.0 nm and monitoring the emission decay at 612.2 nm.

Luminescence properties of sample of $[P_{4448}]_3[EuCl_6]$

1) Emission spectra

Upon excitation at 394.0 nm (25381 cm^{-1}), in the $^5L_6 \leftarrow {}^7F_0$ transition, the sample shows typical narrow Eu^{3+} emission peaks (Fig. S5). The peaks labelled a-e have been assigned to the corresponding electronic transitions in Table S3.

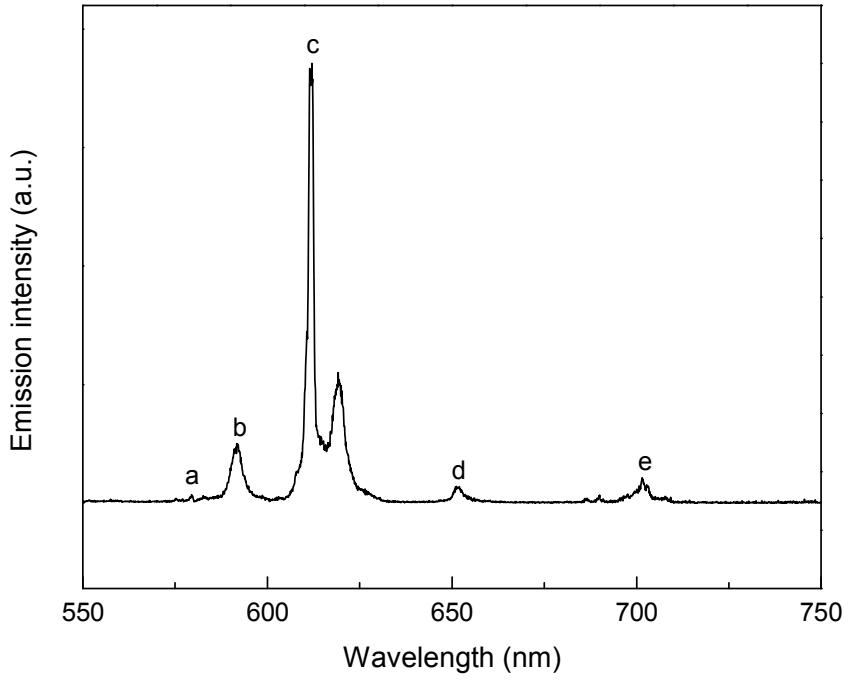

Fig. S5 Emission spectrum of of $[P_{4448}]_3[EuCl_6]$, excited at 394.0 nm and corrected for detector sensitivity.

Table S3. Assignment of the 4f-4f transitions in the emission spectrum of $[P_{4448}]_3[EuCl_6]$.

Label	λ (nm)	$\bar{\upsilon}$ (cm^{-1})	Transition
a	579.5	17256	$^5D_0 \rightarrow {}^7F_0$
b	591.7	16900	$^5D_0 \rightarrow {}^7F_1$
c	612.0	16340	$^5D_0 \rightarrow {}^7F_2$
d	651.3	15354	$^5D_0 \rightarrow {}^7F_3$

e	701.5	14255	$^5D_0 \rightarrow {}^7F_4$

The sample was also excited at 344.9nm (28994 cm^{-1}) giving rise to typical Eu^{3+} peaks as when excited at 394.0 nm, but with slightly lower intensity (Fig. S5 and Fig. S6).

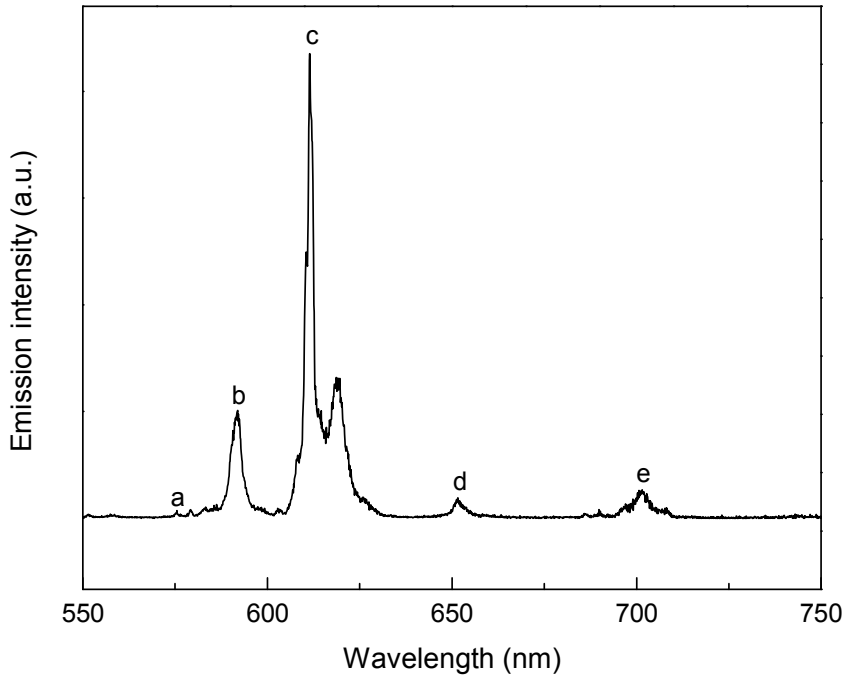

Fig. S6 Emission spectrum of $[P_{4448}]_3[EuCl_6]$, excited at 344.9 nm and corrected for detector sensitivity.

2) Excitation spectrum

Monitoring the emission of the sample at 612.0 nm (16340 cm^{-1}, $^5D_0 \rightarrow {}^7F_2$ transition), the excitation wavelength was varied between 250 and 500 nm to record an excitation spectrum (Fig. S7). In the spectrum a broad band with a maximum at 344.9 nm (28994 cm^{-1})

is visible. All other peaks in the spectrum can be assigned to transitions within the Eu^{3+} ion's 4f shell. The peaks labelled a-i have been assigned to the corresponding transitions in Table S4.

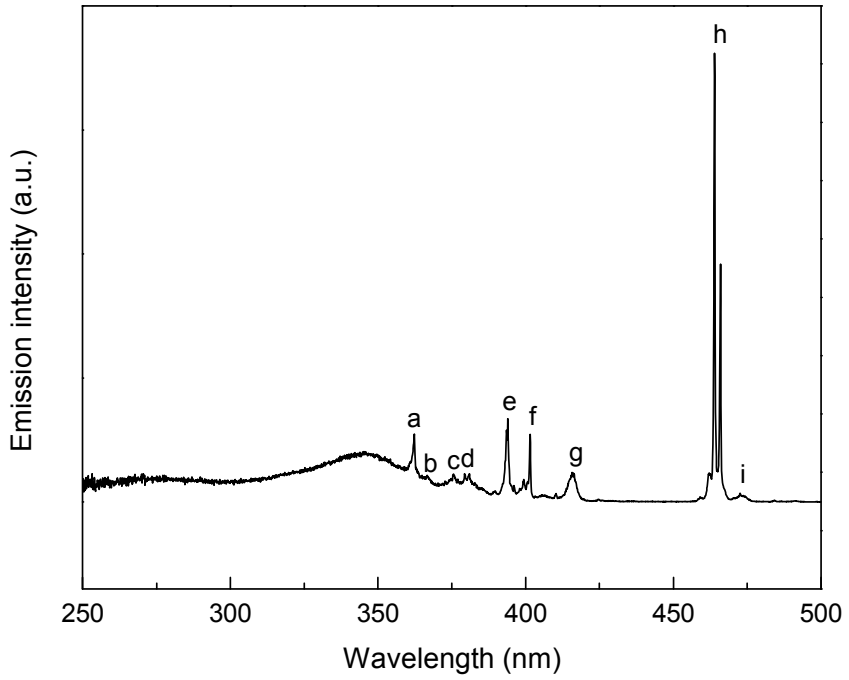

Fig. S7 Excitation spectrum of $[P_{4448}]_3[EuCl_6]$, monitored at 612.0 nm, corrected for detector sensitivity.

Table S4. Assignment of the 4f-4f transitions in the excitation spectrum of $[P_{4448}]_3[EuCl_6]$.

Label	λ (nm)	$\bar{\upsilon}$ (cm^{-1})	Transition
a	362.3	27601	$^5D_4 \leftarrow {}^7F_0$
b	364.9	27405	$^5D_4 \leftarrow {}^7F_1$
c	374.8	26681	$^5G_{6,4} \leftarrow {}^7F_0$
d	379.6	26344	$^5G_{6,5,3} \leftarrow {}^7F_1$
e	394.0	25381	$^5L_6 \leftarrow {}^7F_0$
f	401.4	24913	$^5L_6 \leftarrow {}^7F_1$

g	415.3	24079	$^5D_3 \leftarrow {}^7F_1$
h	464.0	21552	$^5D_2 \leftarrow {}^7F_0$
i	471.4	21213	$^5D_2 \leftarrow {}^7F_1$

3) Luminescence decay time of $[P_{4448}]_3[EuCl_6]$

Upon excitation at 355.0 nm with a pulsed light source, the emission at 612.0 nm shows a mono-exponential decay profile. The luminescence decay profile is given in Fig. S8. The luminescence decay time is calculated as 0.813 ms or 813 µs.

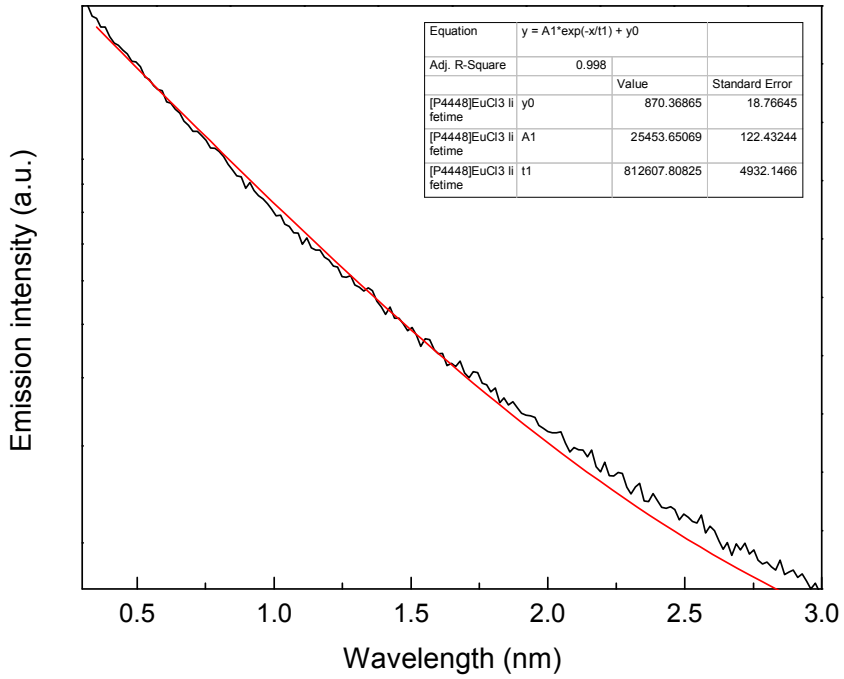

Fig. S8 Luminescence decay profile of $[P_{4448}]_3[EuCl_6]$, upon excitation at 355.0 nm and monitoring the emission decay at 612.0 nm.

Luminescence decay time for $[P_{666\,14}]_3[EuCl_6]$

Upon excitation at 355.0 nm with a pulsed light source, the emission at 611.8 nm shows a mono-exponential decay profile. The luminescence decay profile is given in Fig. S9. The luminescence decay time is calculated as 1.095 ms or 1095 µs.

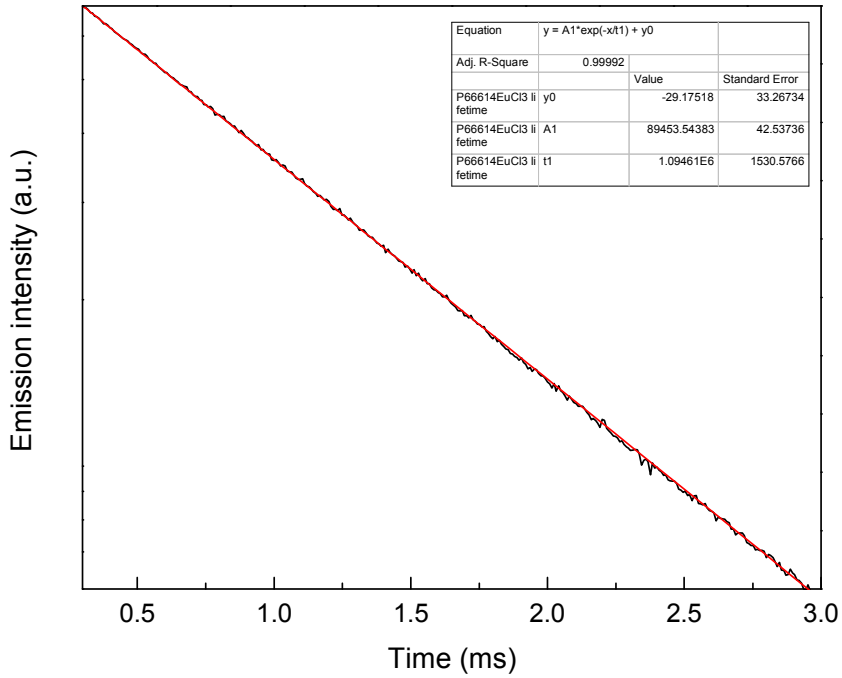

Fig. S9 Luminescence decay profile of $[P_{666\,14}]_3[EuCl_6]$, upon excitation at 355.0 nm and monitoring the emission decay at 611.8 nm.

Luminescence properties of sample $[P_{4444}]_3[TbCl_6]$

1) Emission spectra

Upon excitation at 378.1 nm (26448 cm^{-1}), in the $^5G_6$, $^5D_3 \leftarrow {}^7F_6$ transitions, the sample shows typical narrow Tb^{3+} emission peaks (Fig. S10). The peaks labelled a-d have been assigned to the corresponding electronic transitions in Table S7.

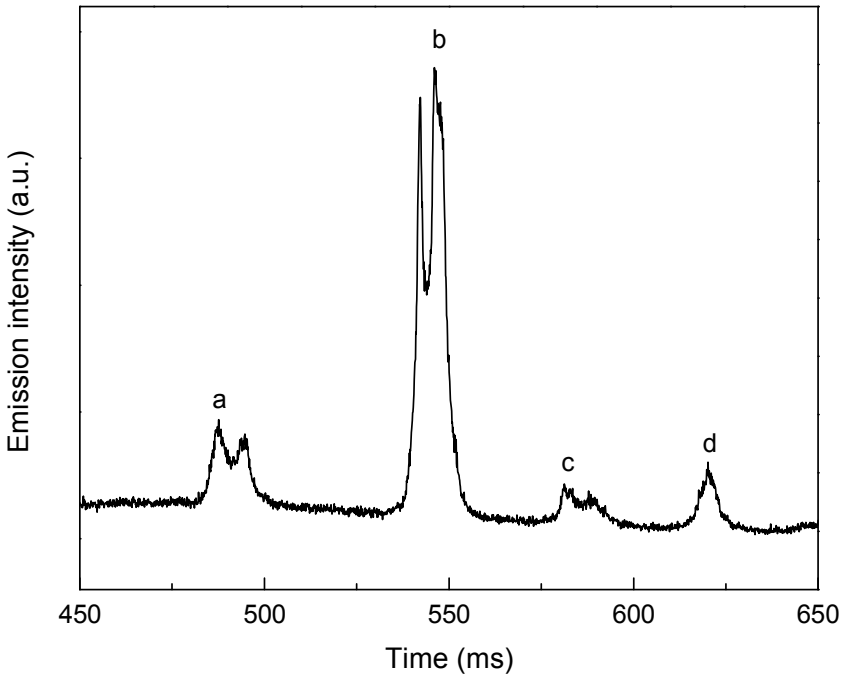

Fig. S10: Emission spectrum of $[P_{4444}]_3[TbCl_6]$, excited at 378.1 nm and corrected for detector sensitivity.

Table S7. Assignment of the 4f-4f transitions in the emission spectrum of $[P_{4444}]_3[TbCl_6]$

Label	λ (nm)	$\bar{\upsilon}$ (cm^{-1})	Transition
a	487.6	20509	$^5D_4 \rightarrow {}^7F_6$
b	546.2	18308	$^5D_4 \rightarrow {}^7F_5$
c	581.3	17203	$^5D_4 \rightarrow {}^7F_4$
d	620.2	16124	$^5D_4 \rightarrow {}^7F_3$

The sample was also excited at 272.5 nm (36697 cm^{-1}) giving rise to typical Tb^{3+} peaks, but more intensive then when excited at 378.1 nm (Fig. S14).

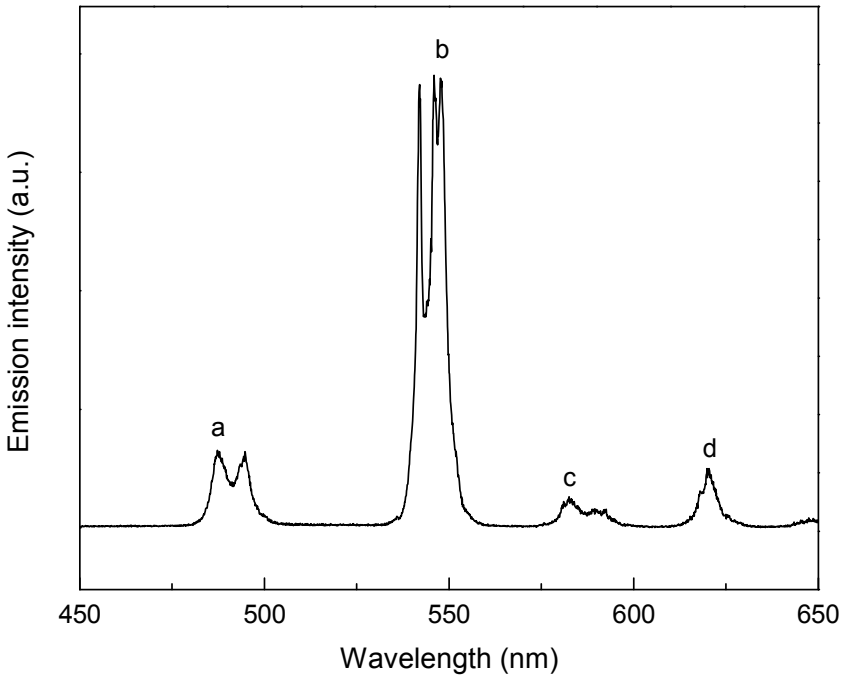

Fig. S14: Emission spectrum of $[P_{4444}]_3[TbCl_6]$, excited at 272.5 nm and corrected for detector.

2) Excitation spectrum of $[P_{4444}]_3[TbCl_6]$

Monitoring the emission of the sample at 546.2 nm (18308 cm^{-1}, $^5D_4 \rightarrow {}^7F_5$ transition), the excitation wavelength was varied between 250 and 500 nm to record an excitation spectrum (Fig. S15). In the spectrum a broad band with a maximum at 272.5 nm (36697 cm^{-1}) is visible. All other peaks in the spectrum can be assigned to transitions within the Tb^{3+} ion's 4f shell. The peaks labelled a-g have been assigned to the corresponding transitions in Table S8.

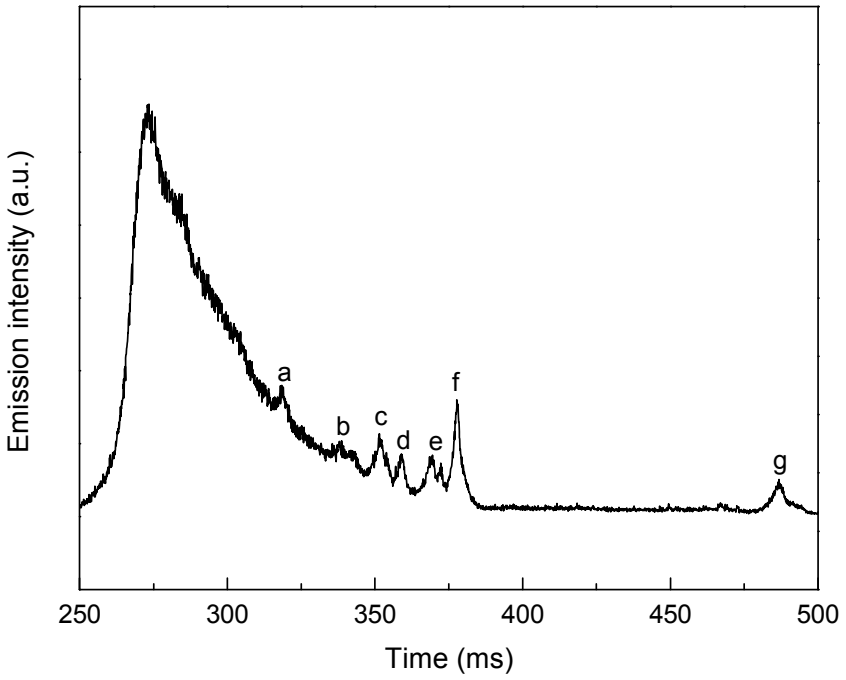

Fig. S15 Excitation spectrum of $[P_{4444}]_3[TbCl_6]$, monitored at 546.2 nm.

Table S8. Assignment of the 4f-4f transitions in the excitation spectrum of $[P_{4444}]_3[TbCl_6]$.

Label	λ (nm)	$\bar{\upsilon}$ (cm^{-1})	Transition
a	318.0	31447	$^5H_7 \leftarrow {}^7F_6$
b	338.8, 341.8	29516, 29257	$^5G_2$, $^5L_6$, $^5L_{7,8}$, $^5G_3 \leftarrow {}^7F_6$
c	351.4	28458	$^5L_9$, $^5G_4$, $^5D_2 \leftarrow {}^7F_6$
d	359.0	27855	$^5G_5 \leftarrow {}^7F_6$
e	369.5	27064	$^5L_{10} \leftarrow {}^7F_6$
f	378.1	26448	$^5G_6$, $^5D_3 \leftarrow {}^7F_6$
g	486.5	20555	$^5D_4 \leftarrow {}^7F_6$

3) Luminescence decay time of $[P_{4444}]_3[TbCl_6]$

Upon excitation at 355.0 nm with a pulsed light source, the emission at 546.2 nm shows a mono-exponential decay profile. The luminescence decay profile is given in Fig. 16. The luminescence decay time is calculated as 0.416 ms or 416 µs.

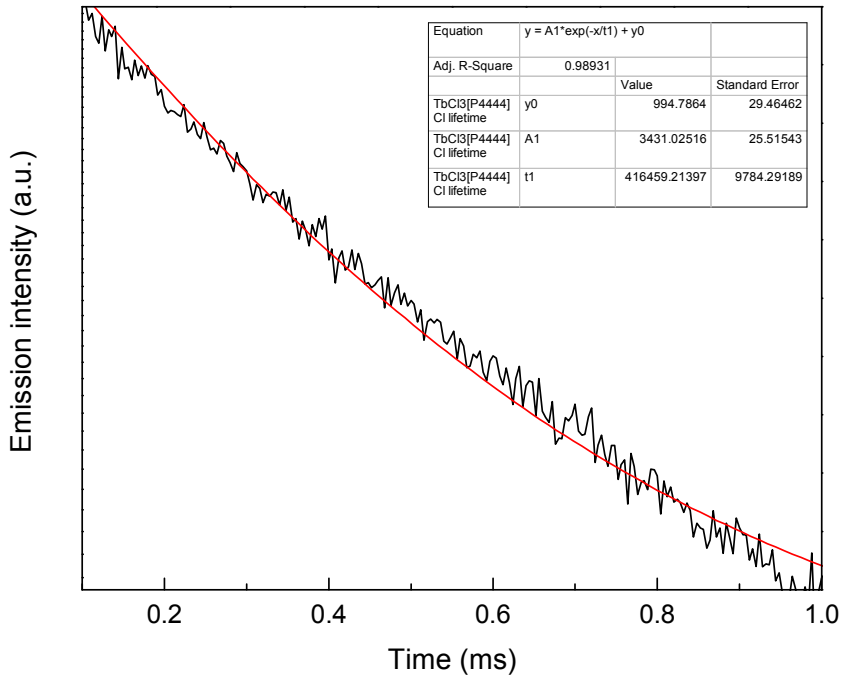

Fig. S16 Luminescence decay profile of $[P_{4444}]_3[TbCl_6]$ upon excitation at 355.0 nm and monitoring the emission decay at 546.2 nm.

Luminescence properties of sample $[P_{4448}]_3[TbCl_6]$

1) Emission spectra

Upon excitation at 377.8 nm (26469 cm^{-1}), in the $^5G_6$, $^5D_3 \leftarrow {}^7F_6$ transitions, the sample shows typical narrow Tb^{3+} emission peaks (Fig. S17). The peaks labelled a-d have been assigned to the corresponding electronic transitions in Table S9.

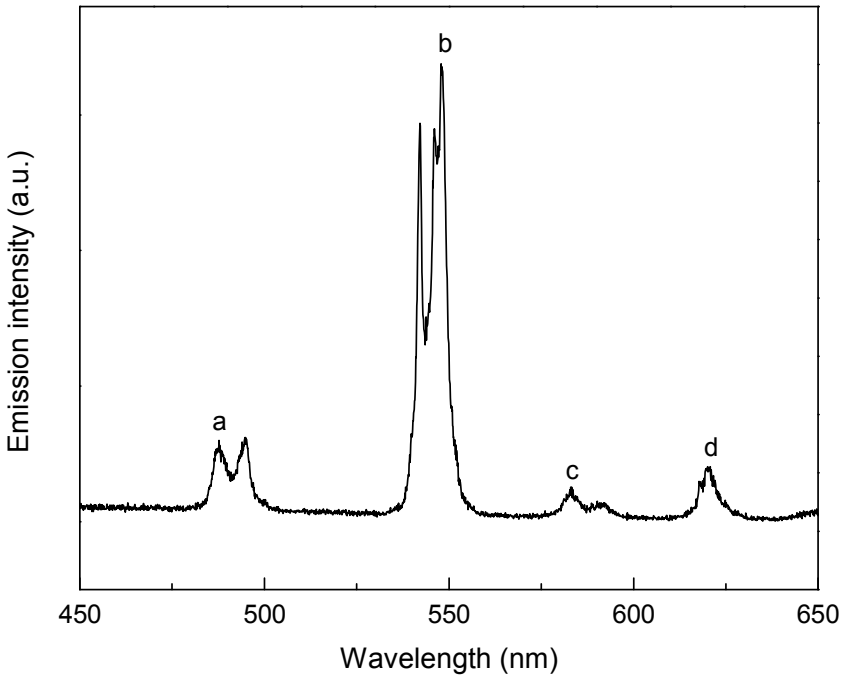

Fig. S17 Emission spectrum of [P4448]3[TbCl6], excited at 377.8 nm and corrected for detector sensitivity.

Table S9. Assignment of the 4f-4f transitions in the emission spectrum of $[P_{4448}]_3[TbCl_6]$

Label	λ (nm)	$\bar{\upsilon}$ (cm^{-1})	Transition
a	487.7	20504	$^5D_4 \rightarrow {}^7F_6$
b	548.0	18248	$^5D_4 \rightarrow {}^7F_5$
c	583.2	17147	$^5D_4 \rightarrow {}^7F_4$
d	620.1	16126	$^5D_4 \rightarrow {}^7F_3$

The sample was also excited at 274.7 nm (36403 cm^{-1}) giving rise to typical Tb^{3+} peaks, but more intensive then when excited at 377.8 nm (Fig. S18).

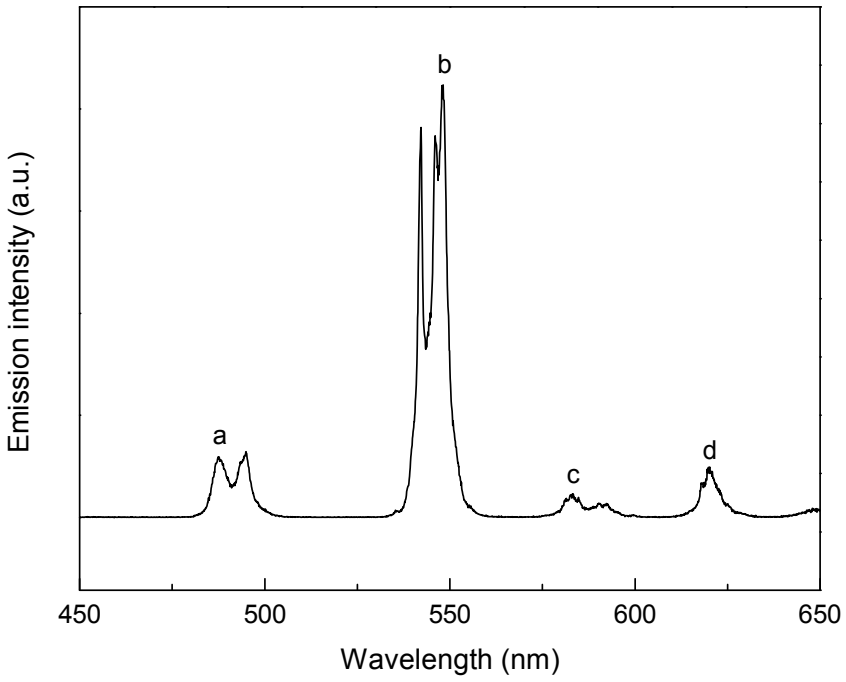

Fig. S18 Emission spectrum of $[P_{4448}]_3[TbCl_6]$, excited at 274.7 nm and corrected for detector sensitivity.

2) Excitation spectrum of $[P_{4448}]_3[TbCl_6]$

Monitoring the emission of the sample at 548.0 nm (18248 cm^{-1}, $^5D_4 \rightarrow {}^7F_5$ transition), the excitation wavelength was varied between 250 and 500 nm to record an excitation spectrum (Fig. 19). In the spectrum a broad band with a maximum at 274.7 nm (36403 cm^{-1}) is visible. All other peaks in the spectrum can be assigned to transitions within the Tb^{3+} ion's 4f shell. The peaks labelled a-h have been assigned to the corresponding transitions in Table S10.

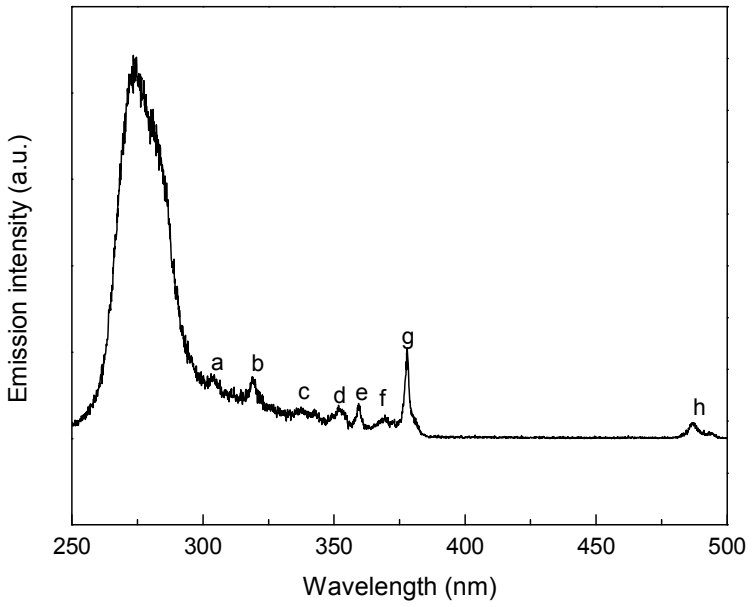

Fig. S19 Excitation spectrum of $[P_{4448}]_3[TbCl_6]$, monitored at 548.0 nm (uncorrected spectrum).

Table S10. Assignment of the 4f-4f transitions in the excitation spectrum of $[P_{4448}]_3[TbCl_6]$.

Label	λ (nm)	$\bar{\upsilon}$ (cm^{-1})	Transition
a	303.8	32916	$^5H_6 \leftarrow {}^7F_6$
b	318.6	31387	$^5H_7 \leftarrow {}^7F_6$
c	337.4, 342.5	29638, 29197	$^5G_2$, $^5L_6$, $^5L_{7,8}$, $^5G_3 \leftarrow {}^7F_6$
d	351.7	28433	$^5L_9$, $^5G_4$, $^5D_2 \leftarrow {}^7F_6$
e	359.3	27832	$^5G_5 \leftarrow {}^7F_6$
f	369.4	27071	$^5L_{10} \leftarrow {}^7F_6$
g	377.8	26469	$^5G_6$, $^5D_3 \leftarrow {}^7F_6$
h	486.9	20538	$^5D_4 \leftarrow {}^7F_6$

3) Luminescence decay time of $[P_{4448}]_3[TbCl_6]$

Upon excitation at 355.0 nm with a pulsed light source, the emission at 548.0 nm shows a mono-exponential decay profile. The luminescence decay profile is given in Fig. S20. The luminescence decay time is calculated as 0.471 ms or 471 µs.

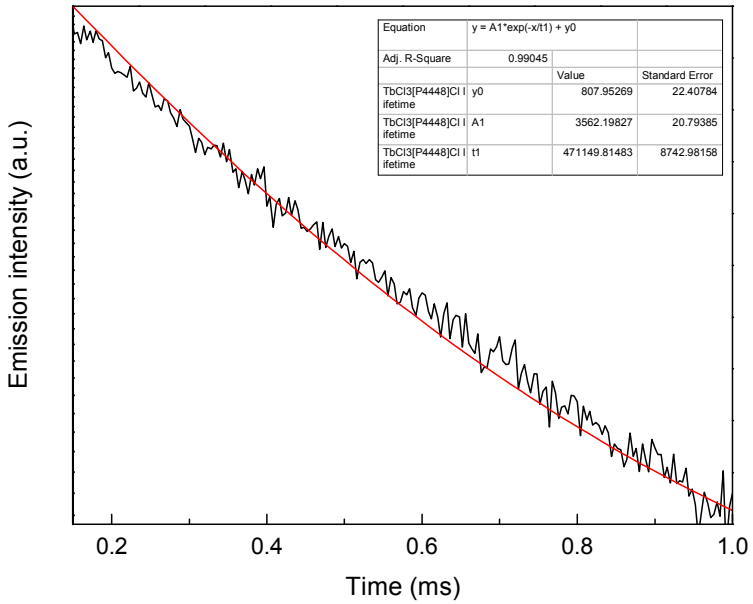

Fig. S20 Luminescence decay profile of $[P_{4448}]_3[TbCl_6]$ upon excitation at 355.0 nm and monitoring the emission decay at 548.0 nm.

Luminescence properties of sample $[P_{666\ 14}]_3[TbCl_6]$

The sample was also excited at 273.2 nm (36603 cm^{-1}) giving rise to typical Tb^{3+} peaks, but more intensive then when excited at 378.1 nm (Fig. S21).

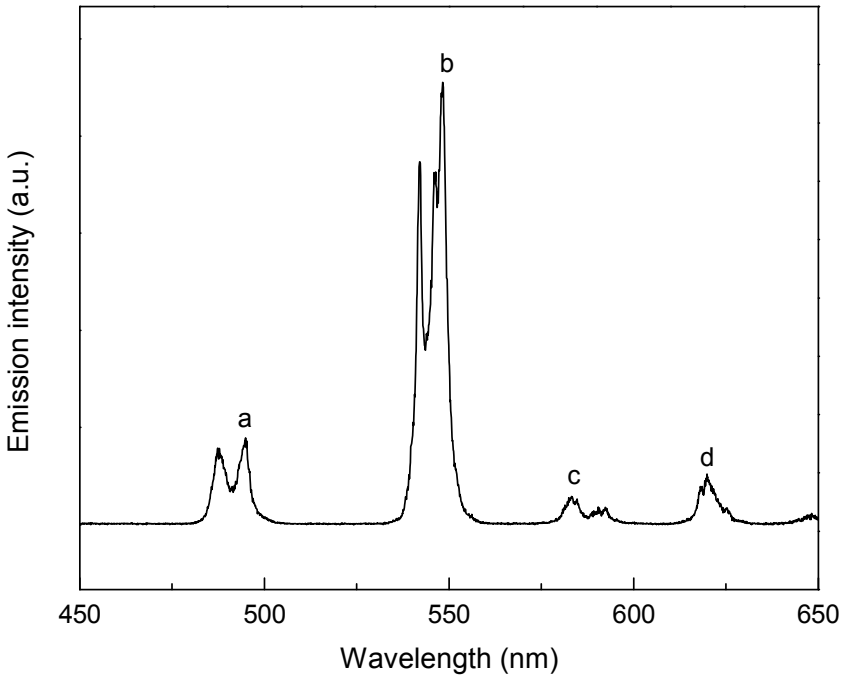

Fig. S21: Emission spectrum of $[P_{666\ 14}]_3[TbCl_6]$, excited at 273.2 nm and corrected for detector sensitivity.

2) Excitation spectrum of $[P_{666\ 14}]_3[TbCl_6]$

Monitoring the emission of the sample at 548.2 nm (18242 cm^{-1}, $^5D_4 \rightarrow {}^7F_5$ transition), the excitation wavelength was varied between 250 and 500 nm to record an excitation spectrum (Fig. S23). In the spectrum a broad band with a maximum at 273.2 nm (36603 cm^{-1}) is visible. All other peaks in the spectrum can be assigned to transitions within the Tb^{3+} ion's 4f shell. The peaks labelled a-i have been assigned to the corresponding transitions in Table S12.

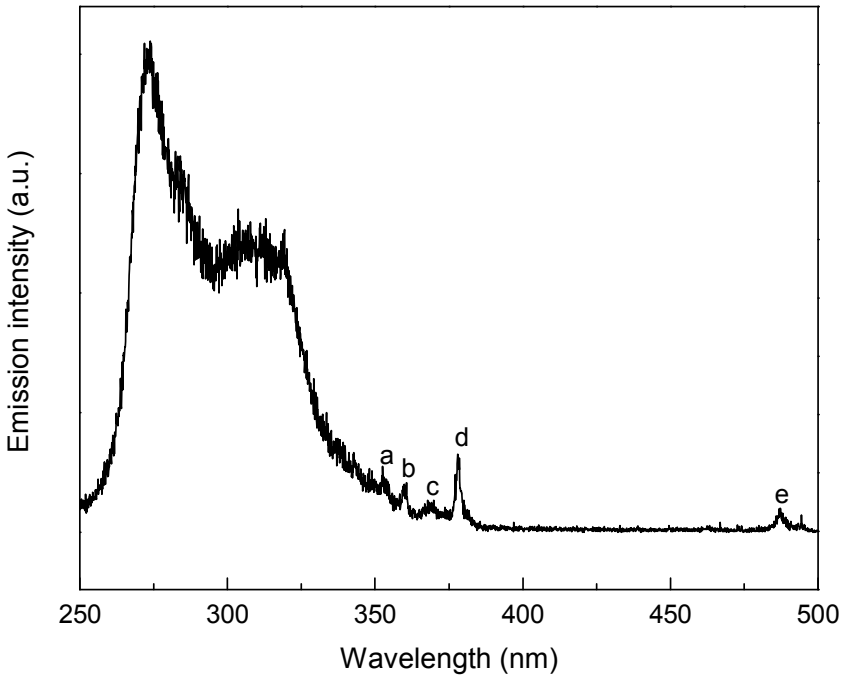

Fig. S23 Excitation spectrum of $[P_{666\,14}]_3[TbCl_6]$, monitored at 548.2 nm (uncorrected spectrum).

Table S12. Assignment of the 4f-4f transitions in the excitation spectrum of $[P_{666\,14}]_3[TbCl_6]$.

Label	λ (nm)	$\bar{\upsilon}$ (cm^{-1})	Transition
a	352.5	28369	$^5L_9 \leftarrow {}^7F_6$
b	360.6	27732	$^5G_5 \leftarrow {}^7F_6$
c	369.8	27042	$^5L_{10} \leftarrow {}^7F_6$
d	378.1	26448	$^5G_6, {}^5D_3 \leftarrow {}^7F_6$
e	487.2	20525	$^5D_4 \leftarrow {}^7F_6$

3) Luminescence decay time of $[P_{666\,14}]_3[TbCl_6]$

Upon excitation at 355.0 nm with a pulsed light source, the emission at 548.2 nm shows a mono-exponential decay profile. The luminescence decay profile is given in Fig. S24. The luminescence decay time is calculated as 0.692 ms or 692 μs.

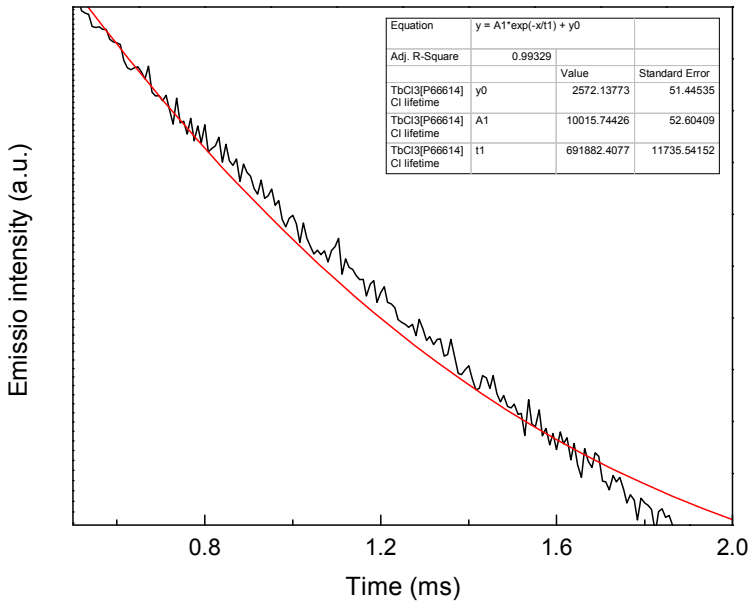

Fig. S24 Luminescence decay profile of $[P_{666\,14}]_3[TbCl_6]$ upon excitation at 355.0 nm and monitoring the emission decay at 548.2 nm.

Luminescence properties of sample $[P_{4444}]_3[DyCl_6]$,

1) Emission spectrum

Upon excitation at 353.2 nm (28313 cm^{-1}), in the $^6P_{7/2} \leftarrow {}^6H_{15/2}$ transition, the sample shows a broad emission band and additionally two typical narrow Dy^{3+} emission peaks (Fig. S25). The peaks labelled a and b have been assigned to the corresponding electronic transitions in Table S13.

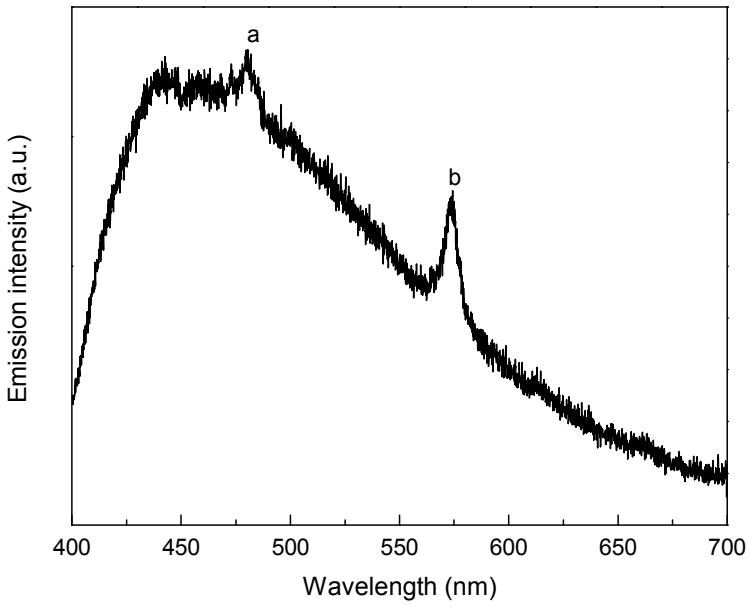

Fig. S25 Emission spectrum of $[P_{4444}]_3[DyCl_6]$, excited at 353.2 nm and corrected for detector sensitivity.

Table S13. Assignment of the 4f-4f transitions in the emission spectrum of $[P_{4444}]_3[DyCl_6]$

Label	λ (nm)	$\bar{\upsilon}$ (cm^{-1})	Transition
a	479.5	20855	$^4F_{9/2} \rightarrow {}^6H_{15/2}$
b	573.4	17440	$^4F_{9/2} \rightarrow {}^6H_{13/2}$

2) Excitation spectrum

Monitoring the emission of the sample at 573.4 nm (17440 cm^{-1}, $^4F_{9/2} \rightarrow {}^6H_{13/2}$ transition), the excitation wavelength was varied between 250 and 480 nm to record an excitation spectrum (Fig. S26). In the spectrum a broad band is visible. All other peaks in the spectrum can be assigned to transitions within the Dy^{3+} ion's 4f shell. The peaks labelled a-i have been assigned to the corresponding transitions in Table S14.

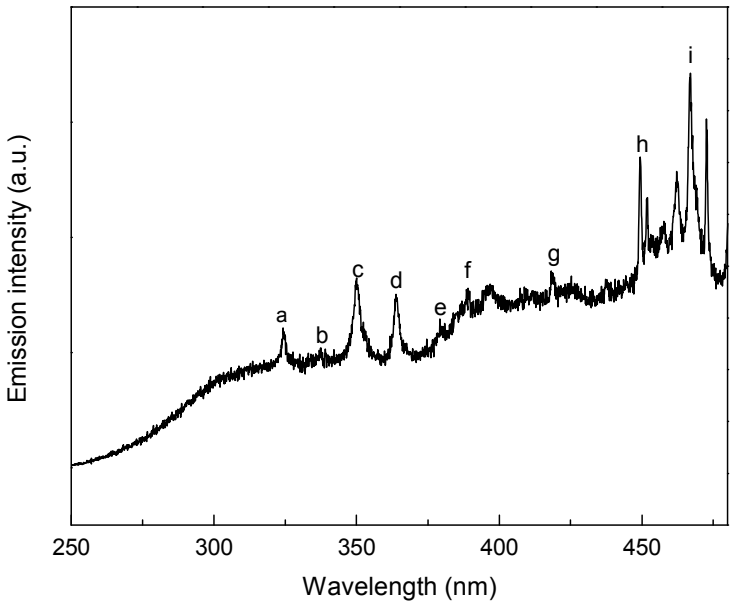

Fig. S26 Excitation spectrum of $[P_{4444}]_3[DyCl_6]$, monitored at 573.4 nm (uncorrected spectrum).

Table S14. Assignment of the 4f-4f transitions in the excitation spectrum of $[P_{4444}]_3[DyCl_6]$.

Label	λ (nm)	$\bar{\upsilon}$ (cm^{-1})	Transition
a	324.3	30845	$^6P_{3/2}\leftarrow{}^6H_{15/2}$
b	337.5	29630	$^4F_{5/2}$, $^4D_{5/2}\leftarrow{}^6H_{15/2}$
c	353.2	28313	$^6P_{7/2}\leftarrow{}^6H_{15/2}$
d	363.7	27495	$^6P_{5/2}$, $^4P_{3/2}$, $^4D_{3/2}$, $^4M_{19/2}$, $\leftarrow{}^6H_{15/2}$
e	379.2	26371	$^4K_{17/2}$, $^4M_{21/2}\leftarrow{}^6H_{15/2}$
f	388.5	25740	$^4I_{13/2}$, $^4F_{7/2}\leftarrow{}^6H_{15/2}$
g	418.2	23912	$^4G_{11/2}\leftarrow{}^6H_{15/2}$
h	449.4	22252	$^4I_{15/2}\leftarrow{}^6H_{15/2}$
i	467.0	21413	$^4F_{9/2}\leftarrow{}^6H_{15/2}$

3) Luminescence decay time of $[P_{4444}]_3[DyCl_6]$

Upon excitation at 355.0 nm with a pulsed light source, the emission at 573.4 nm shows a mono-exponential decay profile. The luminescence decay profile is given in Fig. S27. The luminescence decay time is calculated as 0.055 ms or 55 µs.

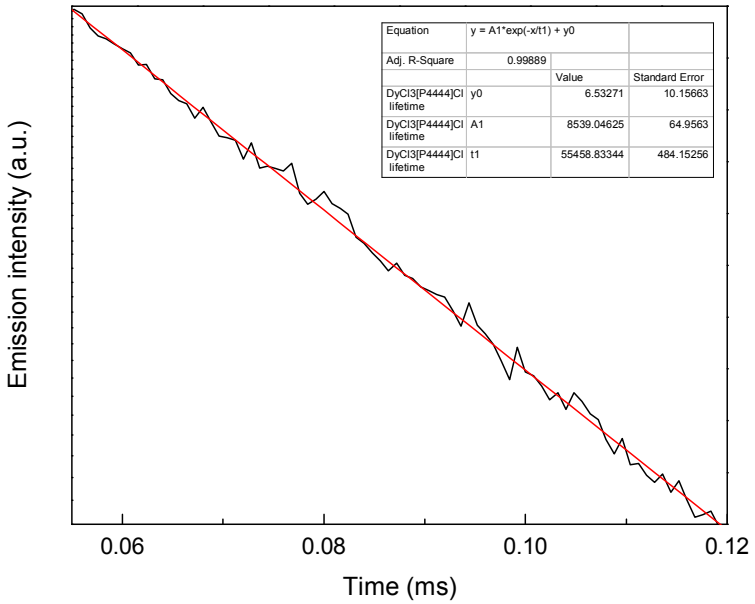

Fig. S27 Luminescence decay profile of $[P_{4444}]_3[DyCl_6]$ upon excitation at 355.0 nm and monitoring the emission decay at 573.4 nm.

Luminescence properties of sample $[P_{4448}]_3[DyCl_6]$

1) Emission spectrum

Upon excitation at 351.1 nm (28482 cm^{-1}), in the $^6P_{7/2} \leftarrow {}^6H_{15/2}$ transition, the sample shows a broad emission band and the three typical narrow Dy^{3+} emission peaks (Fig. 28). One of the peaks (peak a) is strongly overlapped by the broad band and can hardly be distinguished. The peaks labelled a-c have been assigned to the corresponding electronic transitions in Table S15.

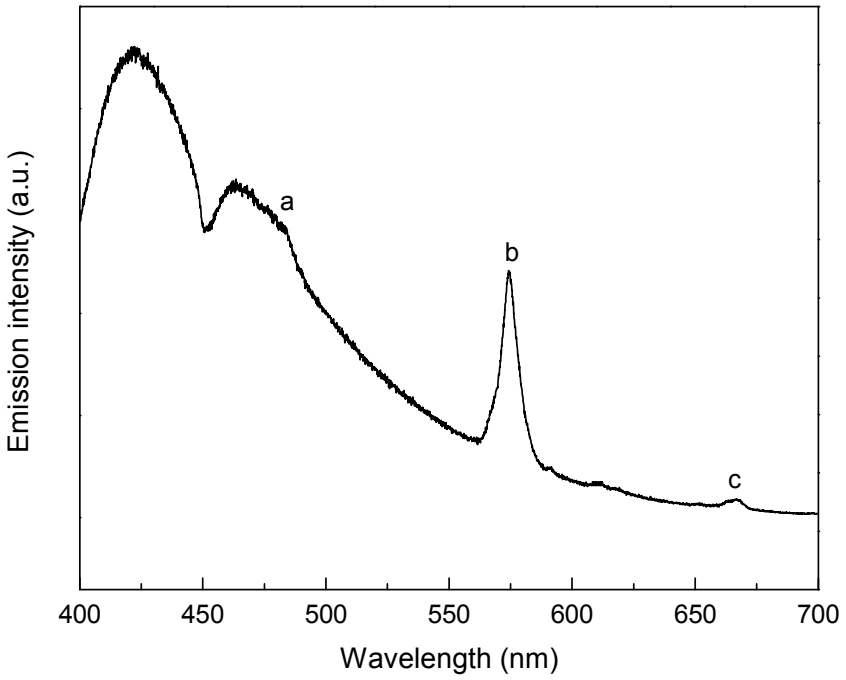

Fig. S28 Emission spectrum of $[P_{4448}]_3[DyCl_6]$, excited at 351.1 nm and corrected for detector sensitivity.

Table S15. Assignment of the 4f-4f transitions in the emission spectrum of $[P_{4448}]_3[DyCl_6]$

Label	λ (nm)	$\bar{\upsilon}$ (cm^{-1})	Transition
a	481.7	20760	$^4F_{9/2}\rightarrow{}^6H_{15/2}$
b	574.5	17406	$^4F_{9/2}\rightarrow{}^6H_{13/2}$
c	666.9	14995	$^4F_{9/2}\rightarrow{}^6H_{11/2}$

2) Excitation spectrum of $[P_{4448}]_3[DyCl_6]$

Monitoring the emission of the sample at 574.5 nm (17406 cm^{-1}, $^4F_{9/2}\rightarrow{}^6H_{13/2}$ transition), the excitation wavelength was varied between 250 and 480 nm to record an excitation spectrum (Fig. S29). In the spectrum a broad band is visible. All other peaks in the spectrum can be assigned to transitions within the Dy^{3+} ion's 4f shell. The peaks labelled a-l have been assigned to the corresponding transitions in Table S16.

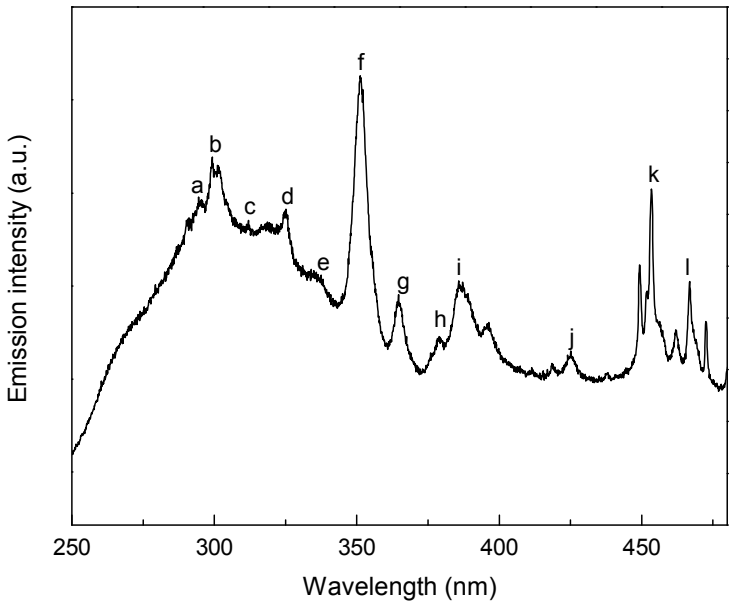

Fig. S29 Excitation spectrum of $[P_{4448}]_3[DyCl_6]$, monitored at 574.5 nm (uncorrected spectrum).

Table S16. Assignment of the 4f-4f transitions in the excitation spectrum of $[P_{4448}]_3[DyCl_6]$.

Label	λ (nm)	$\bar{\upsilon}$ (cm^{-1})	Transition
a	294.5	33956	$^4D_{7/2}\leftarrow{}^6H_{15/2}$
b	299.2	33422	$^4H_{13/2}\leftarrow{}^6H_{15/2}$
c	311.5	32102	$^4L_{19/2}\leftarrow{}^6H_{15/2}$
d	325.1	30760	$^6P_{3/2}\leftarrow{}^6H_{15/2}$
e	337.2	29656	$^4F_{5/2}$, $^4D_{5/2}\leftarrow{}^6H_{15/2}$
f	351.1	28482	$^6P_{7/2}\leftarrow{}^6H_{15/2}$
g	364.7	27420	$^6P_{5/2}$, $^4P_{3/2}$, $^4D_{3/2}$, $^4M_{19/2}\leftarrow{}^6H_{15/2}$
h	378.9	26392	$^4K_{17/2}$, $^4M_{21/2}\leftarrow{}^6H_{15/2}$
i	385.7	25927	$^4I_{13/2}$, $^4F_{7/2}\leftarrow{}^6H_{15/2}$
j	425.1	23528	$^4G_{11/2}\leftarrow{}^6H_{15/2}$

k	453.4	22056	$^4I_{15/2} \leftarrow {}^6H_{15/2}$
l	466.8	21422	$^4F_{9/2} \leftarrow {}^6H_{15/2}$

3) Luminescence decay time of $[P_{4448}]_3[DyCl_6]$

Upon excitation at 355.0 nm with a pulsed light source, the emission at 574.5 nm shows a mono-exponential decay profile. The luminescence decay profile is given in Fig. S30. The luminescence decay time is calculated as 0.056 ms or 56 µs.

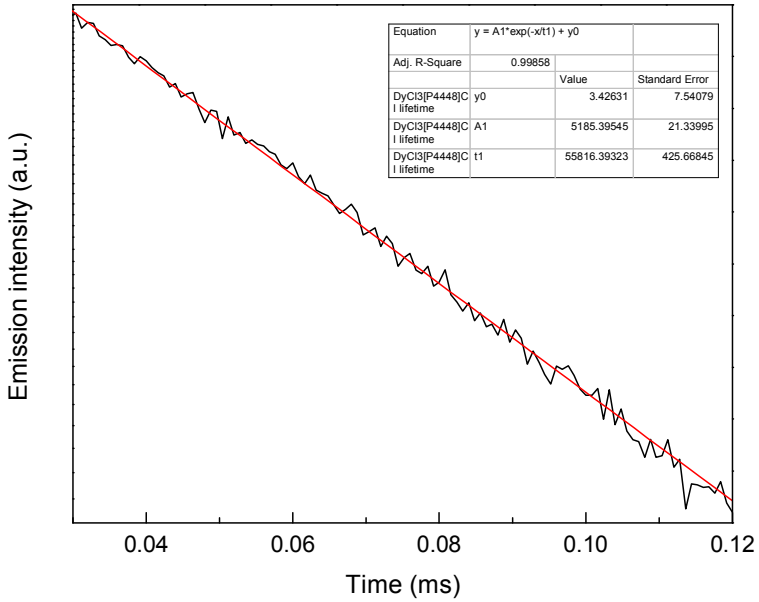

Fig. S30 Luminescence decay profile of $[P_{4448}]_3[DyCl_6]$ upon excitation at 355.0 nm and monitoring the emission decay at 574.5 nm.

Luminescence properties of sample $[P_{4444}]_3[SmCl_6]$

1) Emission spectra

Upon excitation at 400.8 nm (24950 cm^{-1}), in the $^4L_{15/2}$, $^6P_{3/2}$, $^4L_{13/2}\leftarrow{}^6H_{5/2}$ transitions, the sample shows both a broad emission band and the typical narrow Sm^{3+} emission peaks (Fig. S34). The peaks labelled a-d have been assigned to the corresponding electronic transitions in Table S19.

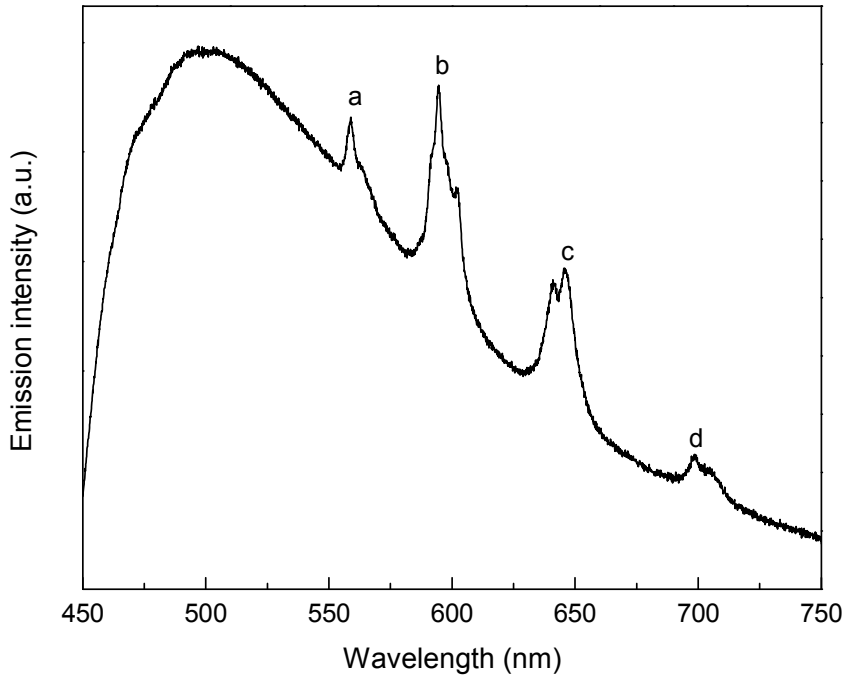

Fig. S34 Emission spectrum of $[P_{4444}]_3[SmCl_6]$, excited at 400.8 nm and corrected for detector sensitivity.

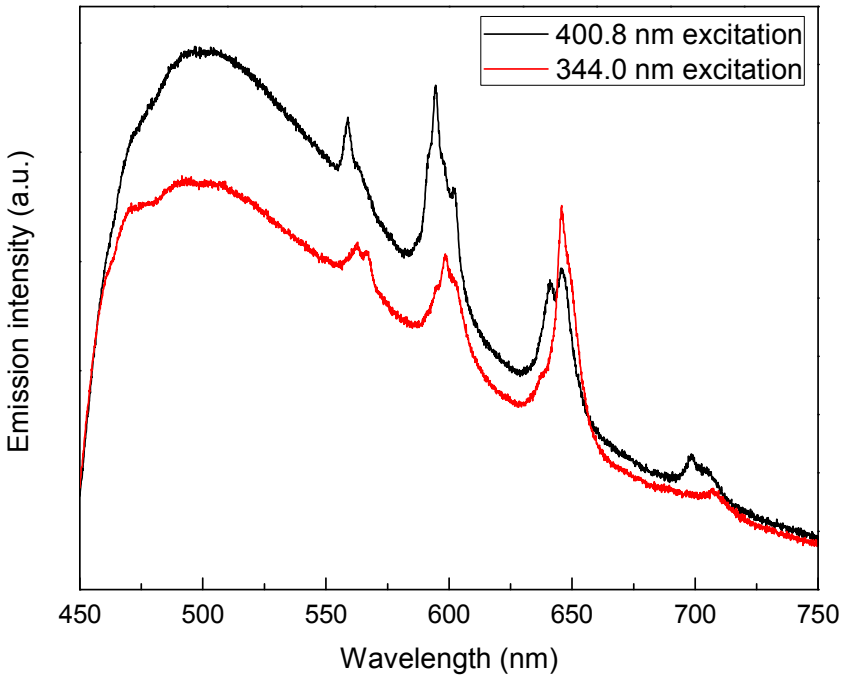

Fig. S34b Comparison of the emission Emission spectra of $[P_{4444}]_3[SmCl_6]$, excited at 400.8 nm (black line) and 344.0 nm (red line) and corrected for detector sensitivity.

Table S19. Assignment of the 4f-4f transitions in the emission spectrum of $[P_{4444}]_3[SmCl_6]$

Label	λ (nm)	$\bar{\upsilon}$ (cm^{-1})	Transition
a	558.8	17895	$^4G_{5/2}\rightarrow{}^6H_{5/2}$
b	594.3	16827	$^4G_{5/2}\rightarrow{}^6H_{7/2}$
c	645.4	15494	$^4G_{5/2}\rightarrow{}^6H_{9/2}$
d	698.4	14318	$^4G_{5/2}\rightarrow{}^6H_{11/2}$

The sample was also excited at 344.0 nm (29070 cm^{-1}) giving rise to typical Sm^{3+} peaks as when excited at 400.8 nm but with lower intensity, except for the $^4G_{5/2}\rightarrow{}^6H_{9/2}$ transition, which is more intensive when the compound is excited at 344.0 nm (Fig. S35 and S35b).

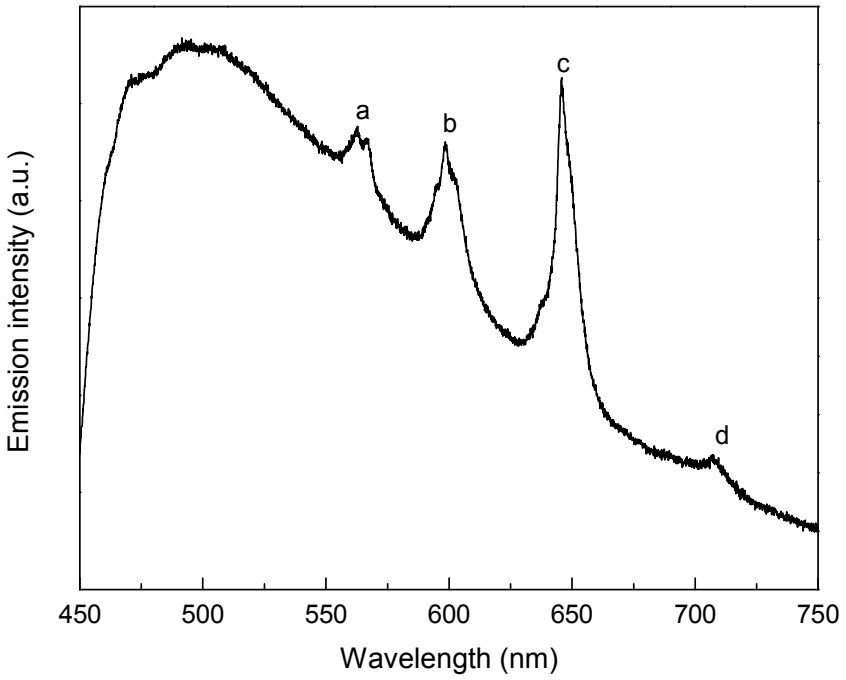

Fig. 35 Emission spectrum of $[P_{4444}]_3[SmCl_6]$, excited at 344.0 nm and corrected for detector sensitivity.

2) Excitation spectrum of $[P_{4444}]_3[SmCl_6]$

Monitoring the emission of the sample at 594.3 nm (16827 cm^{-1}), the excitation wavelength was varied between 250 and 500 nm to record an excitation spectrum (Fig. 36). In the spectrum a broad band is visible. All other peaks in the spectrum can be assigned to transitions within the Sm^{3+} ion's 4f shell. The peaks labelled a-i have been assigned to the corresponding transitions in Table 20.

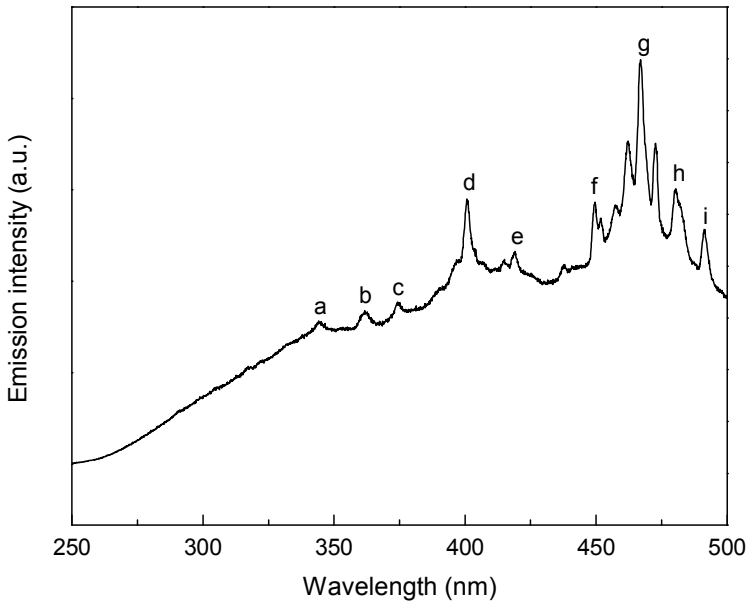

Fig. S36 Excitation spectrum of $[P_{4444}]_3[SmCl_6]$, monitored at 594.3 nm (uncorrected spectrum).

Table S20. Assignment of the 4f-4f transitions in the excitation spectrum of $[P_{4444}]_3[SmCl_6]$.

Label	λ (nm)	$\bar{\upsilon}$ (cm^{-1})	Transition
a	344.9	28994	$^4D_{7/2}$, $^4H_{7/2}\leftarrow{}^6H_{5/2}$
b	361.7	27647	$^4D_{5/2}$, $^6P_{5/2}$, $^4D_{3/2}\leftarrow{}^6H_{5/2}$
c	374.3	26717	$^4K_{13/2}$, $^6P_{7/2}\leftarrow{}^6H_{5/2}$
d	400.8	24950	$^4L_{15/2}$, $^4K_{11/2}$, $^6P_{3/2}$, $^4L_{13/2}\leftarrow{}^6H_{5/2}$
e	418.6	23889	$^6P_{5/2}$, $^4P_{5/2}\leftarrow{}^6H_{5/2}$
f	449.6	22242	$^4G_{9/2}$, $^4M_{17/2}\leftarrow{}^6H_{5/2}$
g	467.0	21413	$^4I_{13/2}\leftarrow{}^6H_{5/2}$
h	480.2	20825	$^4I_{11/2}$, $^4M_{15/2}\leftarrow{}^6H_{5/2}$
i	491.5	20346	$^4I_{9/2}$, $^4G_{7/2}\leftarrow{}^6H_{5/2}$

3) Luminescence decay time of $[P_{4444}]_3[SmCl_6]$

Upon excitation at 355.0 nm with a pulsed light source, the emission at 594.3 nm shows a mono-exponential decay profile. The luminescence decay profile is given in Fig. S37. The luminescence decay time is calculated as 0.026 ms or 26 µs.

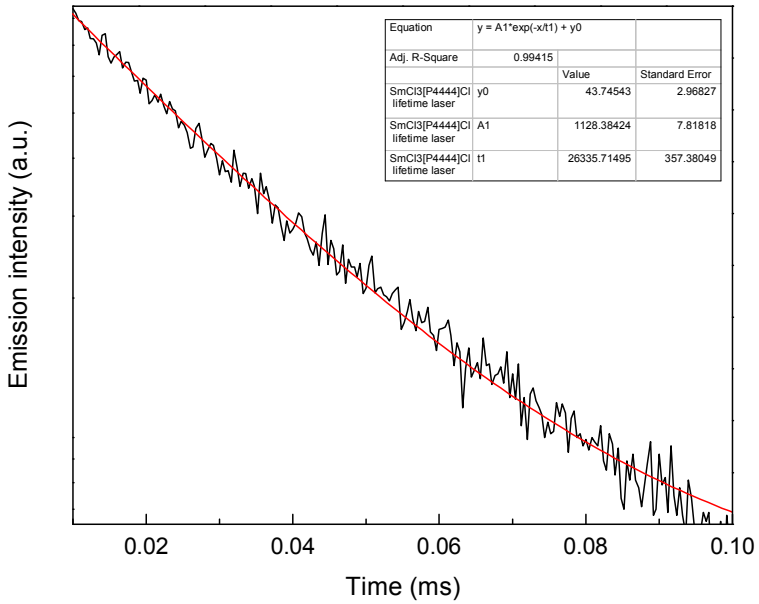

Fig. S37 Luminescence decay profile of $[P_{4444}]_3[SmCl_6]$ upon excitation at 355.0 nm and monitoring the emission decay at 594.3 nm.

Luminescence properties of sample $[P_{4448}]_3[SmCl_6]$

Emission spectra

Upon excitation at 407.0 nm (24570 cm^{-1}), in the $^4L_{15/2}$, $^6P_{3/2}$, $^4L_{13/2} \leftarrow {}^6H_{5/2}$ transitions, the sample shows both a broad emission band and the typical narrow Sm^{3+} emission peaks (Fig. S38). The peaks labelled a-d have been assigned to the corresponding electronic transitions in Table S21.

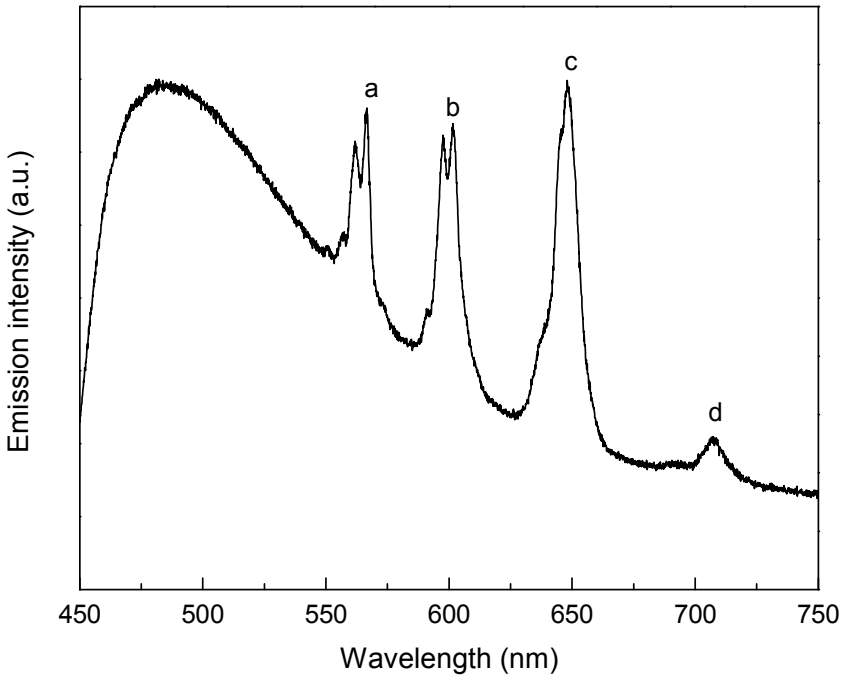

Fig. S38 Emission spectrum of $[P_{4448}]_3[SmCl_6]$, excited at 407.0 nm and corrected for detector sensitivity.

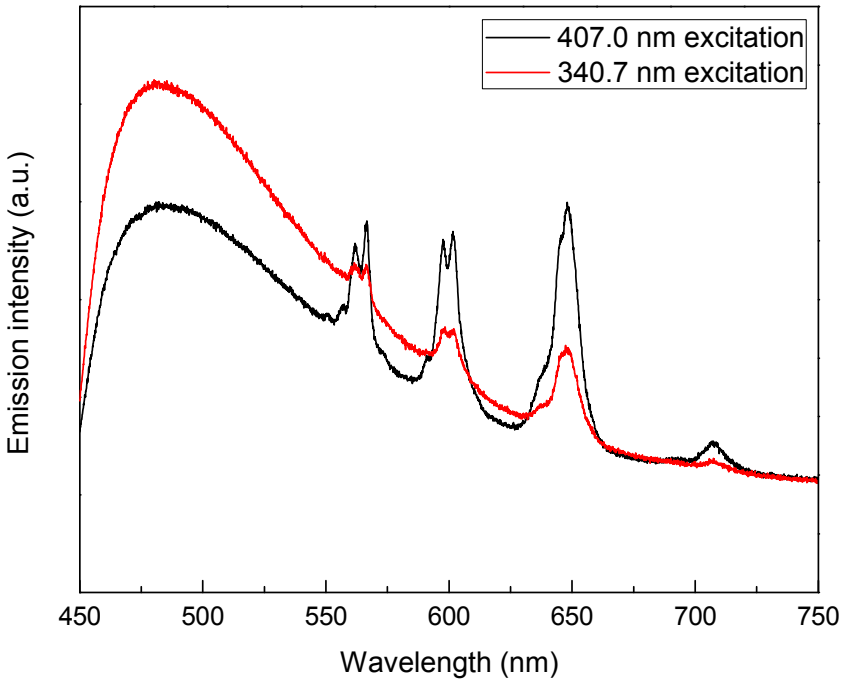

Fig. S38b Comparison of the emission spectra of $[P_{4448}]_3[SmCl_6]$, excited at 407.0 nm (black line) and 340.7 nm (red line) and corrected for detector sensitivity.

Table S21. Assignment of the 4f-4f transitions in the emission spectrum of $[P_{4448}]_3[SmCl_6]$

Label	λ (nm)	$\bar{\upsilon}$ (cm^{-1})	Transition
a	566.7	17646	$^4G_{5/2} \rightarrow {}^6H_{5/2}$
b	601.8	16617	$^4G_{5/2} \rightarrow {}^6H_{7/2}$
c	648.1	15430	$^4G_{5/2} \rightarrow {}^6H_{9/2}$
d	705.3	14178	$^4G_{5/2} \rightarrow {}^6H_{11/2}$

The sample was also excited at 340.7 nm (29351 cm^{-1}), but in this case the sample gave only very weak Sm^{3+} emission peaks with a strong dominance of a wide broad band between 450-550 nm.

2) Excitation spectrum for $[P_{4448}]_3[SmCl_6]$

Monitoring the emission of the sample at 601.8 nm (16617 cm^{-1}), the excitation wavelength was varied between 250 and 500 nm to record an excitation spectrum (Fig. S39). In the spectrum a broad band is visible. All other peaks in the spectrum can be assigned to transitions within the Sm^{3+} ion's 4f shell. The peaks labelled a-i have been assigned to the corresponding transitions in Table S22.

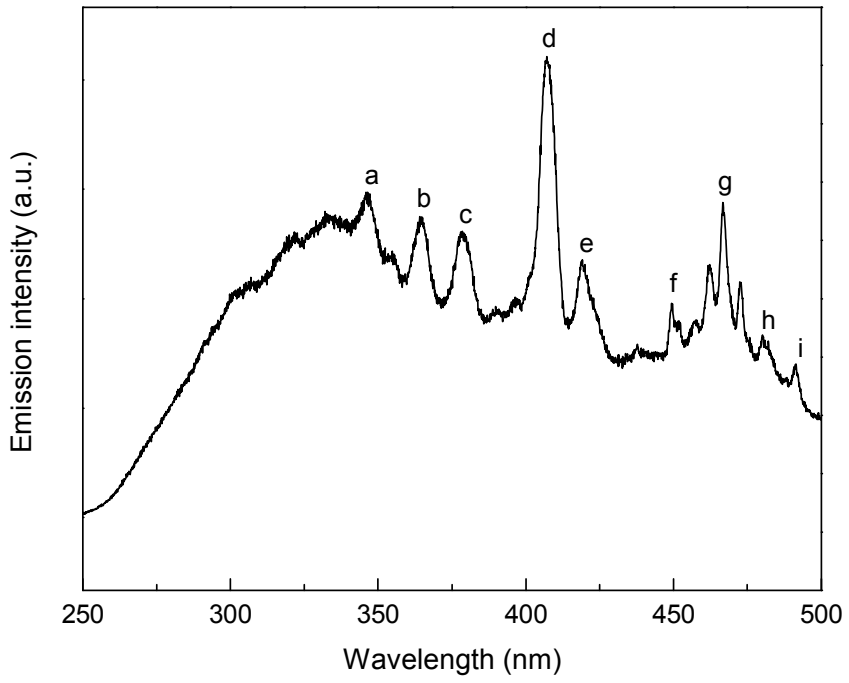

Fig. S39 Excitation spectrum of $[P_{4448}]_3[SmCl_6]$, monitored at 601.8 nm (uncorrected spectrum).

Table S22. Assignment of the 4f-4f transitions in the excitation spectrum of $[P_{4448}]_3[SmCl_6]$.

Label	λ (nm)	$\bar{\upsilon}$ (cm^{-1})	Transition
a	346.0	28902	$^4D_{7/2}$, $^4H_{7/2}\leftarrow{}^6H_{5/2}$
b	364.1	27465	$^4D_{5/2}$, $^6P_{5/2}$, $^4D_{3/2}\leftarrow{}^6H_{5/2}$

c	378.5	26420	$^4K_{13/2}$, $^6P_{7/2}$←$^6H_{5/2}$
d	407.0	24570	$^4L_{15/2}$, $^4K_{11/2}$, $^6P_{3/2}$, $^4L_{13/2}$←$^6H_{5/2}$
e	418.8	23878	$^6P_{5/2}$, $^4P_{5/2}$←$^6H_{5/2}$
f	449.7	22237	$^4G_{9/2}$, $^4M_{17/2}$←$^6H_{5/2}$
g	466.7	21427	$^4I_{13/2}$←$^6H_{5/2}$
h	480.1	20829	$^4I_{11/2}$, $^4M_{15/2}$←$^6H_{5/2}$
i	490.6	20385	$^4I_{9/2}$, $^4G_{7/2}$←$^6H_{5/2}$

3) Luminescence decay time of $[P_{4448}]_3[SmCl_6]$

Upon excitation at 355.0 nm with a pulsed light source, the emission at 601.8 nm shows a mono-exponential decay profile. The luminescence decay profile is given in Fig. S40. The luminescence decay time is calculated as 0.057 ms or 57 µs.

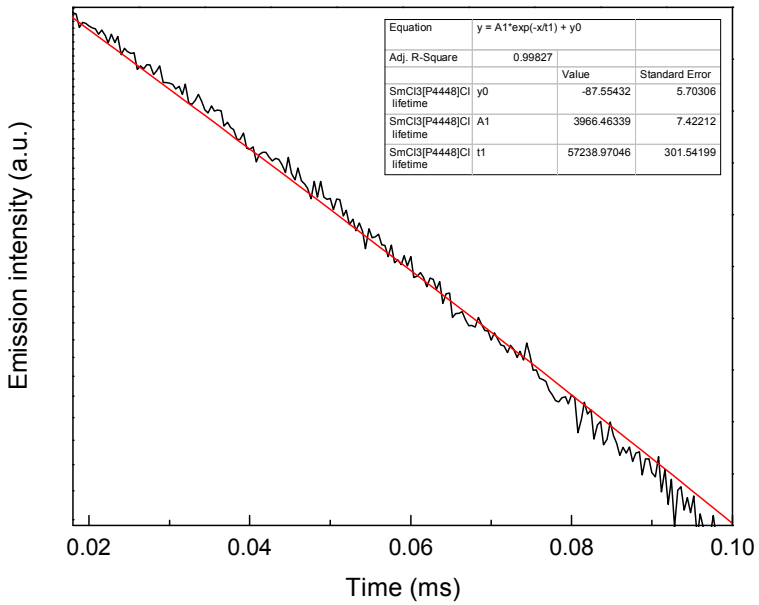

Fig. S40 Luminescence decay profile of $[P_{4448}]_3[SmCl_6]$ upon excitation at 355.0 nm and monitoring the emission decay at 601.8 nm.

Luminescence properties of sample $[P_{666\ 14}]_3[SmCl_6]$

1) Emission spectra

Upon excitation at 407.1 nm (24564 cm^{-1}), in the $^4L_{15/2}$, $^6P_{3/2}$, $^4L_{13/2}\leftarrow{}^6H_{5/2}$ transitions, the sample shows a strong broad emission band and much weaker peaks which can be assigned to the typical narrow Sm^{3+} emission peaks (Fig. S41). The peaks labelled a-d have been assigned to the corresponding electronic transitions in Table S23.

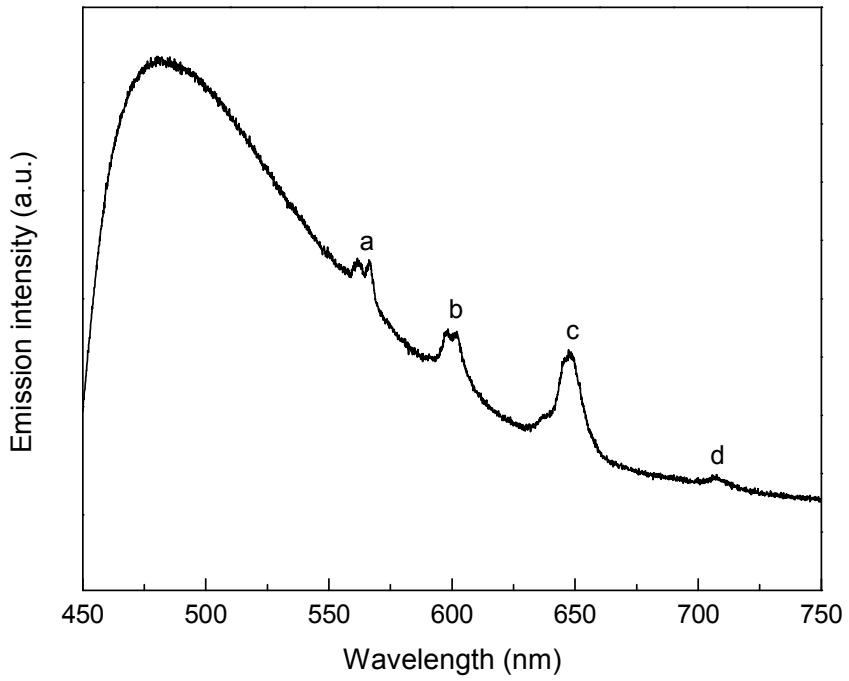

Fig. S41 Emission spectrum of $[P_{666\ 14}]_3[SmCl_6]$, excited at 407.1 nm and corrected for detector sensitivity.

Table S23. Assignment of the 4f-4f transitions in the emission spectrum of $[P_{666\ 14}]_3[SmCl_6]$

Label	λ (nm)	$\bar{\upsilon}$ (cm^{-1})	Transition

a	566.5	17668	$^4G_{5/2} \rightarrow {}^6H_{5/2}$
b	599.0	16694	$^4G_{5/2} \rightarrow {}^6H_{7/2}$
c	647.3	15449	$^4G_{5/2} \rightarrow {}^6H_{9/2}$
d	707.5	14134	$^4G_{5/2} \rightarrow {}^6H_{11/2}$

The sample was also excited at 337.1 nm (29665 cm^{-1}) giving rise to typical Sm^{3+} peaks as when excited at 407.1 nm, but with slightly higher intensity of the peaks (Fig. S42).

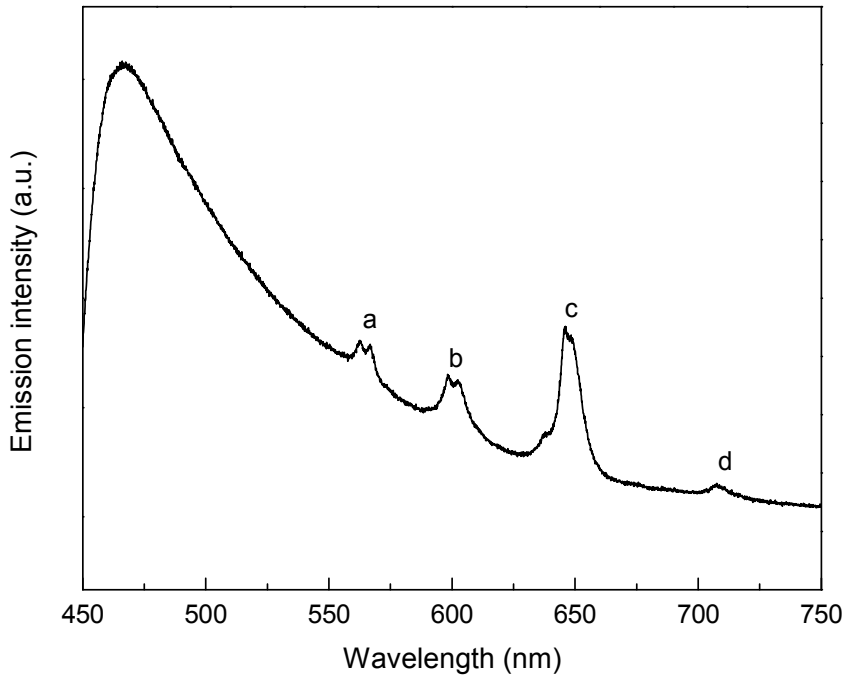

Fig. S42 Emission spectrum of $[P_{666\ 14}]_3[SmCl_6]$, excited at 337.1 nm and corrected for detector sensitivity.

2) Excitation spectrum of $[P_{666\ 14}]_3[SmCl_6]$

Monitoring the emission of the sample at 599.0 nm (16694 cm^{-1}), the excitation wavelength was varied between 250 and 500 nm to record an excitation spectrum (Fig. S43). In the spectrum a broad band is visible. All other peaks in the spectrum can be assigned to transitions within the Sm^{3+} ion's 4f shell. The peaks labelled a-i have been assigned to the corresponding transitions in Table S24.

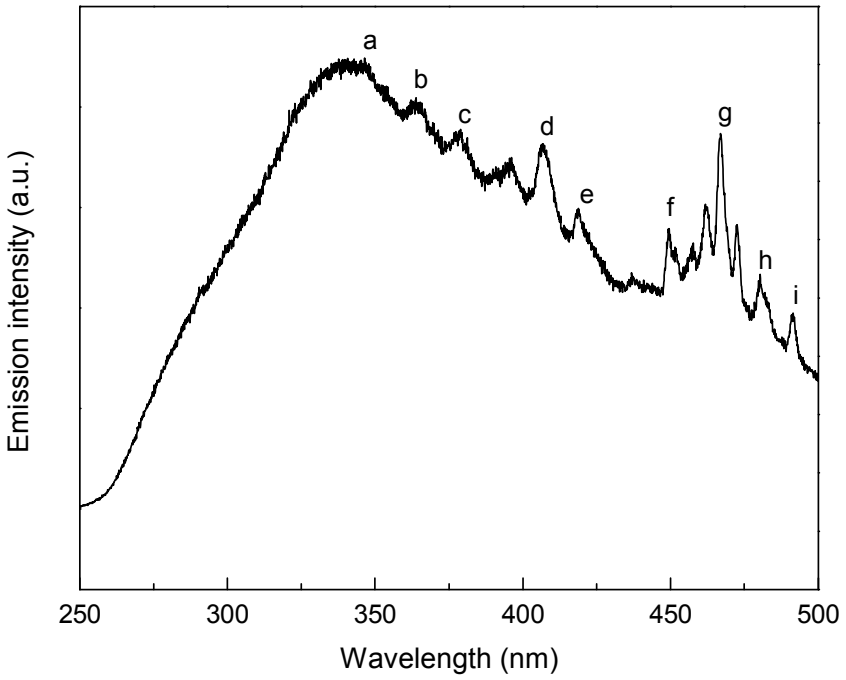

Fig. S43 Excitation spectrum of $[P_{666\ 14}]_3[SmCl_6]$, monitored at 599.0 nm (uncorrected spectrum).

Table S24. Assignment of the 4f-4f transitions in the excitation spectrum of $[P_{666\ 14}]_3[SmCl_6]$.

Label	λ (nm)	$\bar{\upsilon}$ (cm^{-1})	Transition
a	346.4	28868	$^4D_{7/2}$, $^4H_{7/2}\leftarrow{}^6H_{5/2}$
b	363.9	27480	$^4D_{5/2}$, $^6P_{5/2}$, $^4D_{3/2}\leftarrow{}^6H_{5/2}$
c	378.9	26392	$^4K_{13/2}$, $^6P_{7/2}\leftarrow{}^6H_{5/2}$
d	407.1	24564	$^4L_{15/2}$, $^4K_{11/2}$, $^6P_{3/2}$, $^4L_{13/2}\leftarrow{}^6H_{5/2}$
e	418.4	23901	$^6P_{5/2}$, $^4P_{5/2}\leftarrow{}^6H_{5/2}$
f	449.2	22262	$^4G_{9/2}$, $^4M_{17/2}\leftarrow{}^6H_{5/2}$
g	467.0	21413	$^4I_{13/2}\leftarrow{}^6H_{5/2}$
h	480.3	20820	$^4I_{11/2}$, $^4M_{15/2}\leftarrow{}^6H_{5/2}$
i	490.9	20371	$^4I_{9/2}$, $^4G_{7/2}\leftarrow{}^6H_{5/2}$

3) Luminescence decay time of $[P_{666\ 14}]_3[SmCl_6]$

Upon excitation at 355.0 nm with a pulsed light source, the emission at 599.0 nm shows a mono-exponential decay profile. The luminescence decay profile is given in Fig. S44. The luminescence decay time is calculated as 0.033 ms or 33 µs.

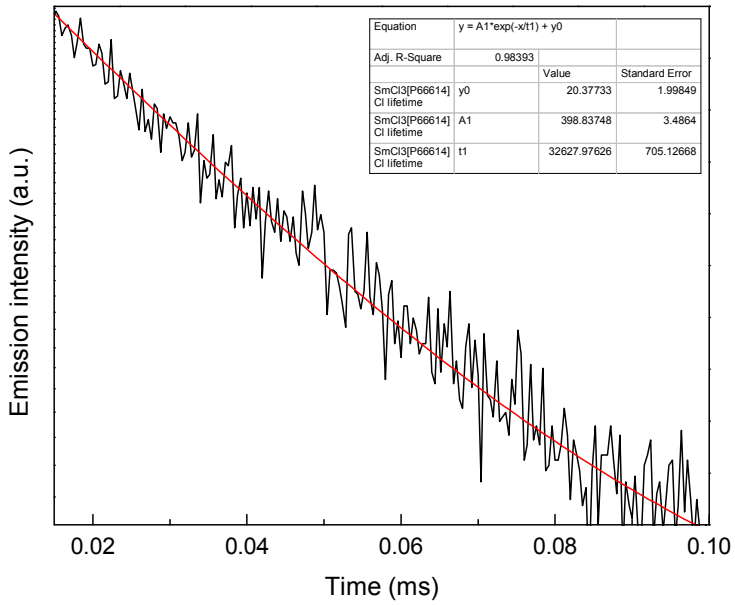

Fig. S44 Luminescence decay profile of $[P_{666\ 14}]_3[SmCl_6]$ upon excitation at 355.0 nm and monitoring the emission decay at 599.0 nm.

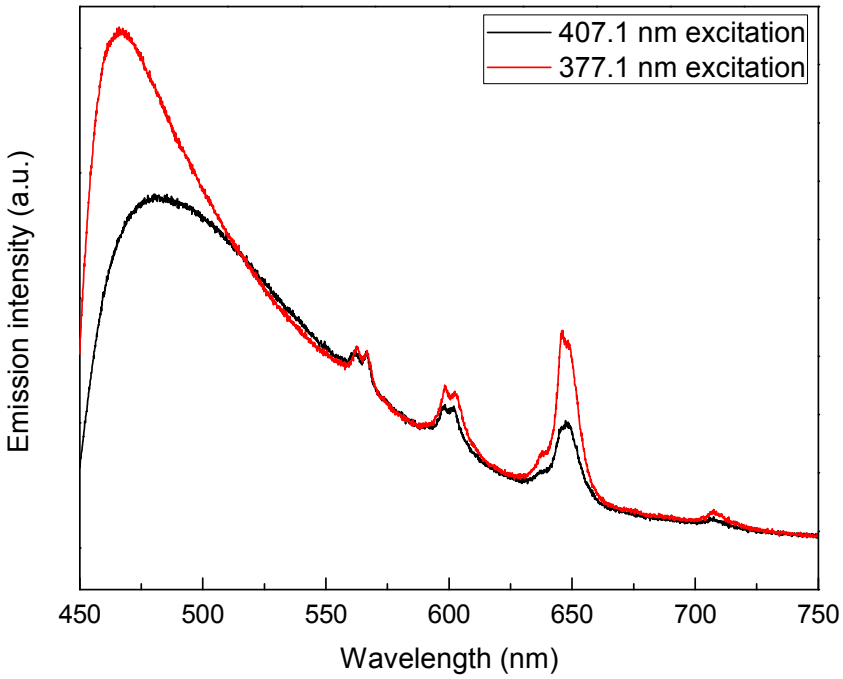

Fig. S44b Comparison of the emission spectra of $[P_{66614}]_3[SmCl_6]$, excited at 407.1 nm (black line) and 377.1 nm (red line) and corrected for detector sensitivity.

Luminescence properties of sample $[P_{666\,14}]_3[CeCl_6]$

1) Emission spectra

Upon excitation at 331.2 nm (30193 cm^{-1}), the sample shows a strong broad band with a maximum at 358.5 nm (27894 cm^{-1}), and a shoulder with a maximum at 394.1 nm (25374 cm^{-1}) (Fig. 51). Additional broad bands are visible in the spectrum.

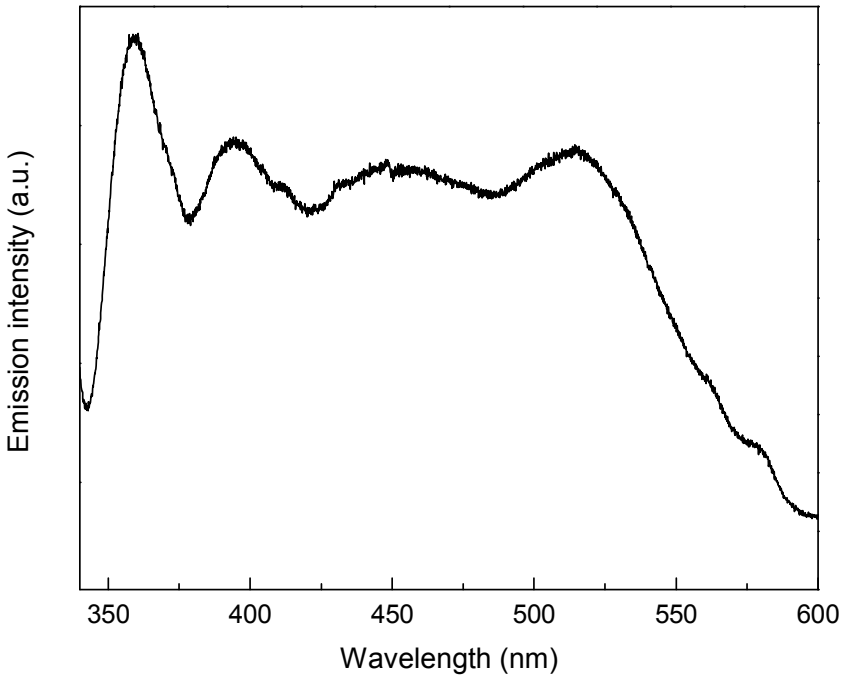

Fig. S51 Emission spectrum of $[P_{666\,14}]_3[CeCl_6]$, excited at 331.2 nm and corrected for detector sensitivity.

2) Excitation spectrum of $[P_{666\,14}]_3[CeCl_6]$

Monitoring the emission of the sample at 394.1 nm (25374 cm^{-1}) the excitation wavelength was varied between 250 nm and 380 nm to record an excitation spectrum (Fig. S52). In the spectrum a broad band with a maximum at 331.2 nm is visible.

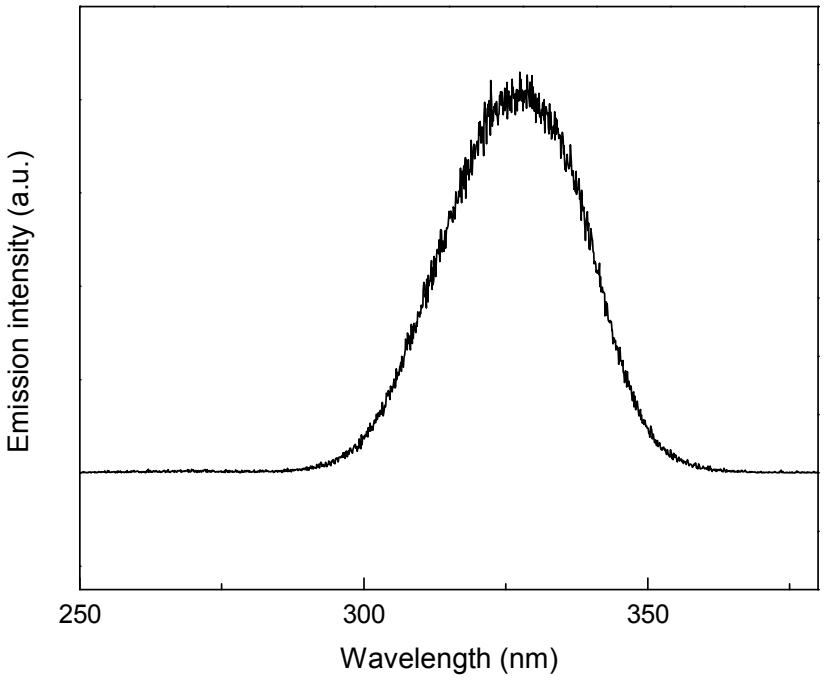

Fig. S52 Excitation spectrum of $[P_{666\ 14}]_3[CeCl_6]$, monitored at 394.1 nm (uncorrected spectrum).

3) Luminescence decay time of $[P_{666\ 14}]_3[CeCl_6]$

Upon excitation at 331.2 nm with a pulsed light source, the emission at 394.1 nm shows a mono-exponential decay profile. The luminescence decay profile is given in Fig. S53. The luminescence decay time is calculated as 0.597 μs or 597 ns.

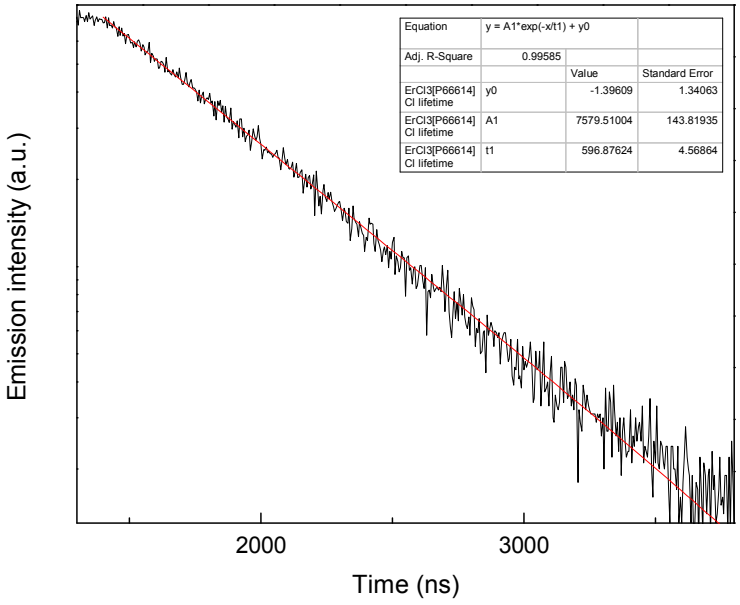

Fig. S53 Luminescence decay profile of $[P_{666\,14}]_3[CeCl_6]$ upon excitation at 331.2 nm and monitoring the emission decay at 394.1 nm.

Luminescence properties of sample $[P_{4444}]_3[NdCl_6]$

1) Emission spectra

Upon excitation at 580.0 nm (17241 cm^{-1}), in the $^2G_{7/2}$, $^4G_{5/2} \leftarrow {}^4I_{9/2}$ transition, the sample shows typical narrow Nd^{3+} emission peaks (Fig. 54). The peaks labelled a-c have been assigned to the corresponding electronic transitions in Table S25.

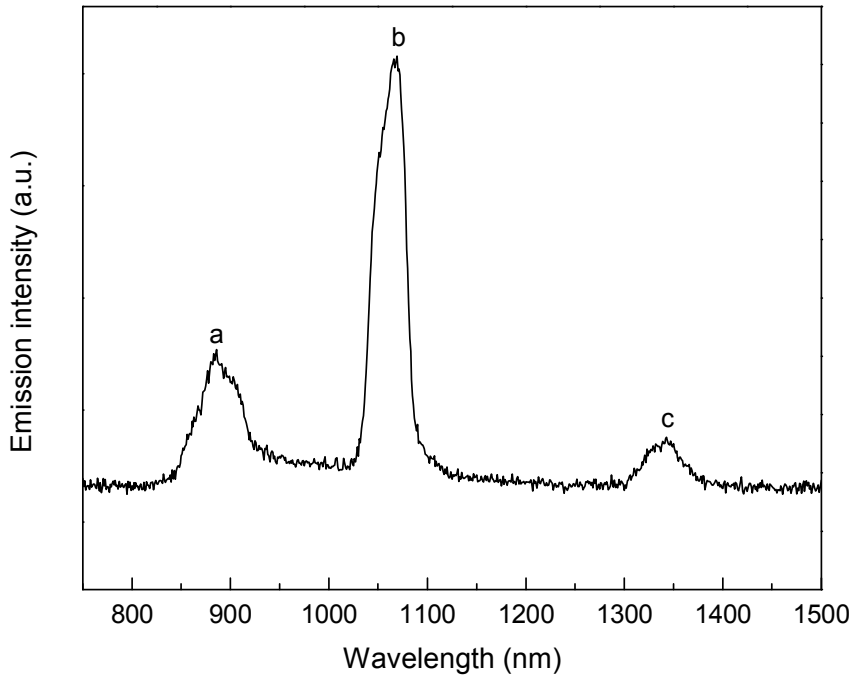

Fig. S54 Emission spectrum of $[P_{4444}]_3[NdCl_6]$, excited at 580.0 nm (uncorrected spectrum).

Table S25. Assignment of the 4f-4f transitions in the emission spectrum of $[P_{4444}]_3[NdCl_6]$.

Label	λ (nm)	$\bar{\upsilon}$ (cm^{-1})	Transition
a	886.0	11287	$^4F_{3/2}\rightarrow{}^4I_{9/2}$
b	1065.0	9390	$^4F_{3/2}\rightarrow{}^4I_{11/2}$
c	1343.0	7446	$^4F_{3/2}\rightarrow{}^4I_{13/2}$

2) Excitation spectrum of $[P_{4444}]_3[NdCl_6]$

Monitoring the emission of the sample at 1065.0 nm (9390 cm^{-1}, $^4F_{3/2}\rightarrow{}^4I_{11/2}$ transition), the excitation wavelength was varied between 250 and 850 nm to record an excitation spectrum (Fig. S55). All the peaks in the spectrum can be assigned to transitions within the Nd^{3+} ion's 4f shell. The peaks labelled a-i have been assigned to the corresponding transitions in Table S26.

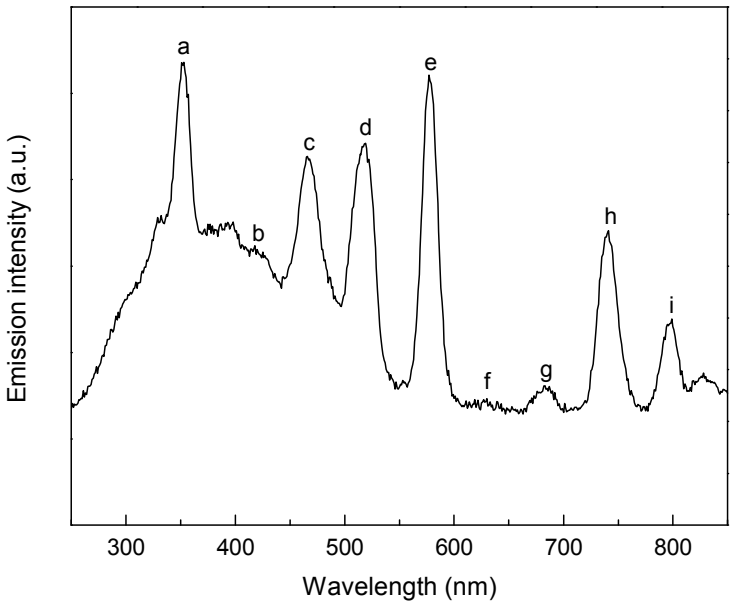

Fig. S55 Excitation spectrum of $[P_{4444}]_3[NdCl_6]$, monitored at 1065.0 nm (uncorrected spectrum).

Table S26. Assignment of the 4f-4f transitions in the excitation spectrum of $[P_{4444}]_3[NdCl_6]$.

Label	λ (nm)	$\bar{\upsilon}$ (cm^{-1})	Transition
a	351.0	28490	$^2L_{15/2}$, $^4D_{1/2}$, $^2I_{11/2}$, $^4D_{5/2}$, $^4D_{3/2} \leftarrow {}^4I_{9/2}$
b	406.0	24631	$^2D_{5/2}$, $^2P_{1/2} \leftarrow {}^4I_{9/2}$
c	465.0	21505	$^4G_{11/2}$, $^2D_{3/2}$, $^2P_{3/2}$, $^2G_{9/2}$, $^2K_{15/2} \leftarrow {}^4I_{9/2}$
d	518.0	19305	$^4G_{9/2}$, $^4G_{7/2}$, $^2K_{13/2} \leftarrow {}^4I_{9/2}$
e	580.0	17241	$^2G_{7/2}$, $^4G_{5/2} \leftarrow {}^4I_{9/2}$
f	629.0	15898	$^2H_{11/2} \leftarrow {}^4I_{9/2}$
g	682.0	14663	$^4F_{9/2} \leftarrow {}^4I_{9/2}$
h	741.0	13495	$^4S_{3/2}$, $^4F_{7/2} \leftarrow {}^4I_{9/2}$
i	797.0	12547	$^2H_{9/2}$, $^4F_{5/2} \leftarrow {}^4I_{9/2}$

3) Luminescence decay times

Upon excitation at 355.0 nm with a pulsed light source, the emission at 1065.0 nm shows a mono-exponential decay profile. The luminescence decay profile is given in Fig. S56. The luminescence decay time is calculated as 1.575 µs or 1575 ns.

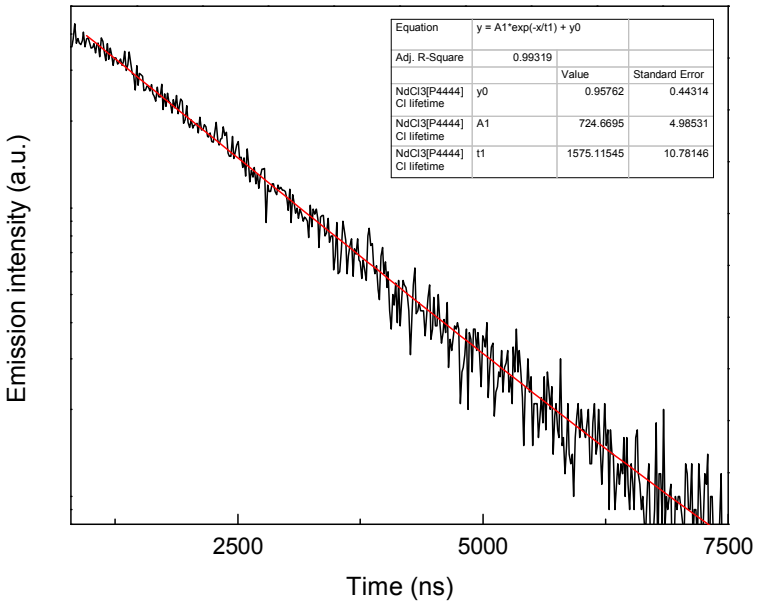

Fig. S56 Luminescence decay profile of $[P_{4444}]_3[NdCl_6]$ upon excitation at 355.0 nm and monitoring the emission decay at 1065.0 nm.

Luminescence properties of sample $[P_{4448}]_3[NdCl_6]$

1) Emission spectra

Upon excitation at 582.0 nm (17182 cm^{-1}), in the $^2G_{7/2}$, $^4G_{5/2} \leftarrow {}^4I_{9/2}$ transition, the sample shows typical narrow Nd^{3+} emission peaks (Fig. S57). The peaks labelled a-c have been assigned to the corresponding electronic transitions in Table S27.

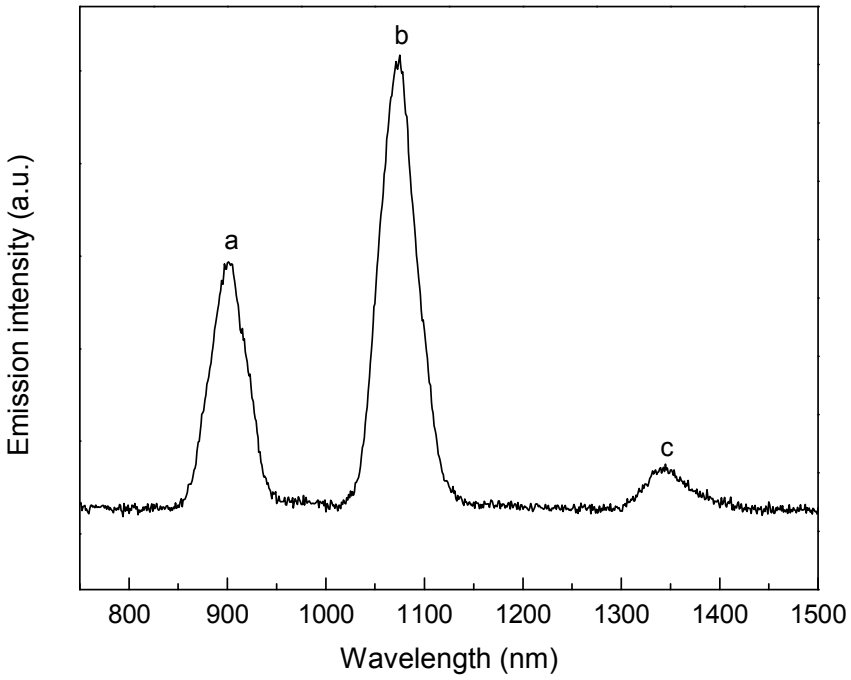

Fig. S57 Emission spectrum of $[P_{4448}]_3[NdCl_6]$, excited at 582.0 nm (uncorrected spectrum).

Table S27. Assignment of the 4f-4f transitions in the emission spectrum of $[P_{4448}]_3[NdCl_6]$.

Label	λ (nm)	$\bar{\upsilon}$ (cm^{-1})	Transition
a	897.0	11148	$^4F_{3/2}\rightarrow{}^4I_{9/2}$
b	1063.0	9390	$^4F_{3/2}\rightarrow{}^4I_{11/2}$
c	1336.0	7485	$^4F_{3/2}\rightarrow{}^4I_{13/2}$

2) Excitation spectrum of $[P_{4448}]_3[NdCl_6]$

Monitoring the emission of the sample at 1065.0 nm (9390 cm^{-1}, $^4F_{3/2}\rightarrow{}^4I_{11/2}$ transition), the excitation wavelength was varied between 250 and 850 nm to record an excitation spectrum (Fig. S58). All the peaks in the spectrum can be assigned to transitions within the Nd^{3+} ion's 4f shell. The peaks labelled a-g have been assigned to the corresponding transitions in Table S28.

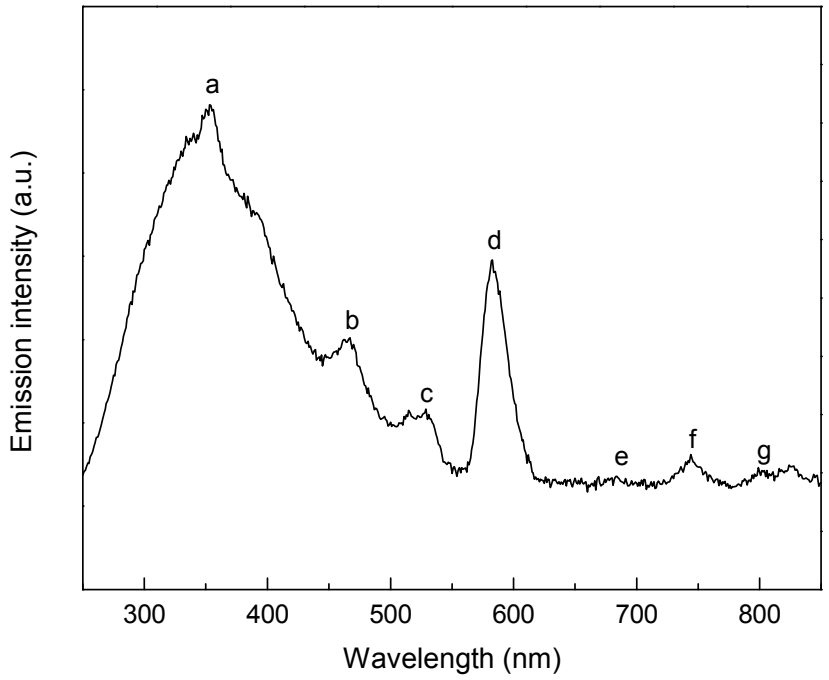

Fig. S58 Excitation spectrum of $[P_{4448}]_3[NdCl_6]$, monitored at 1065.0 nm (uncorrected spectrum).

Table S28. Assignment of the 4f-4f transitions in the excitation spectrum of $[P_{4448}]_3[NdCl_6]$.

Label	λ (nm)	$\bar{\upsilon}$ (cm^{-1})	Transition
a	353.0	28329	$^2L_{15/2}$, $^4D_{1/2}$, $^2I_{11/2}$, $^4D_{5/2}$, $^4D_{3/2} \leftarrow {}^4I_{9/2}$
b	467.0	21413	$^4G_{11/2}$, $^2D_{3/2}$, $^2P_{3/2}$, $^2G_{9/2}$, $^2K_{15/2} \leftarrow {}^4I_{9/2}$
c	526.0	19011	$^4G_{9/2}$, $^4G_{7/2}$, $^2K_{13/2} \leftarrow {}^4I_{9/2}$
d	582.0	17182	$^2G_{7/2}$, $^4G_{5/2} \leftarrow {}^4I_{9/2}$
e	682.0	14663	$^4F_{9/2} \leftarrow {}^4I_{9/2}$
f	744.0	13441	$^4S_{3/2}$, $^4F_{7/2} \leftarrow {}^4I_{9/2}$
g	799.0	12516	$^2H_{9/2}$, $^4F_{5/2} \leftarrow {}^4I_{9/2}$

3) Luminescence decay times

Upon excitation at 355.0 nm with a pulsed light source, the emission at 1065.0 nm shows a mono-exponential decay profile. The luminescence decay profile is given in Fig. S59. The luminescence decay time is calculated as 2.470 µs or 2470 ns.

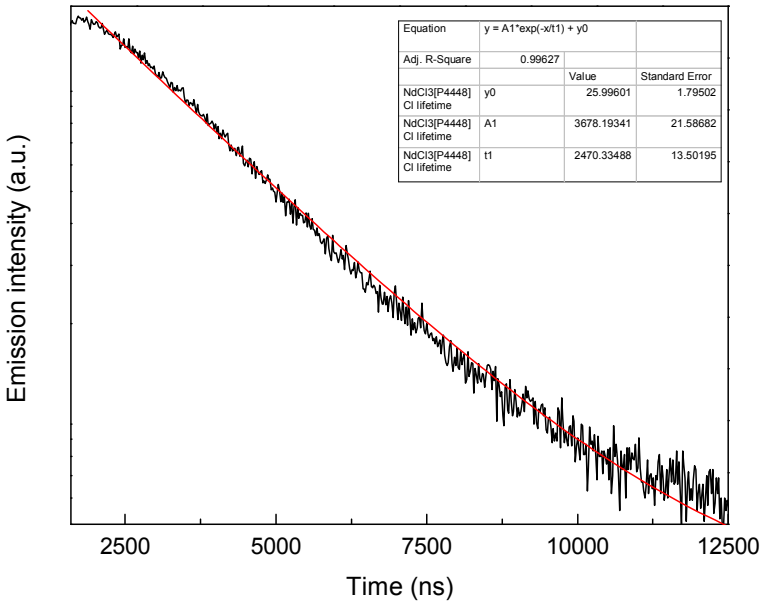

Fig. S59 Luminescence decay profile of $[P_{4448}]_3[NdCl_6]$ upon excitation at 355.0 nm and monitoring the emission decay at 1065.0 nm.

Luminescence properties of sample $[P_{666\ 14}]_3[NdCl_6]$

Luminescence decay times $[P_{666\ 14}]_3[NdCl_6]$

Upon excitation at 355.0 nm with a pulsed light source, the emission at 1064.0 nm shows a mono-exponential decay profile. The luminescence decay profile is given in Fig. S62. The luminescence decay time is calculated as 2.470 µs or 2470 ns.

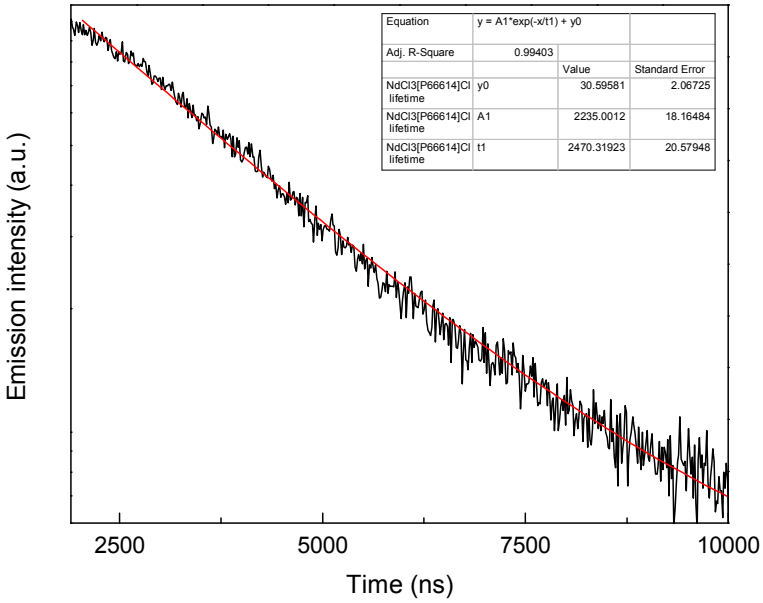

Fig. S62 Luminescence decay profile of $[P_{666\,14}]_3[NdCl_6]$ upon excitation at 355.0 nm and monitoring the emission decay at 1064.0 nm.

Luminescence properties of sample $[P_{4444}]_3[ErCl_6]$

1) Emission spectra

Upon excitation at 355.0 nm (28169 cm^{-1}), in the $^4G_{11/2} \leftarrow {}^4I_{15/2}$ transition, the sample shows only one narrow emission peak of Er^{3+} (Fig. S63). This peak, with a maximum at 1545.0 nm (6472 cm^{-1}), can be assigned to the $^4I_{13/2} \rightarrow {}^4I_{15/2}$ "telecom" transition. The emission was very weak and 20 scans were needed to record the spectrum presented below.

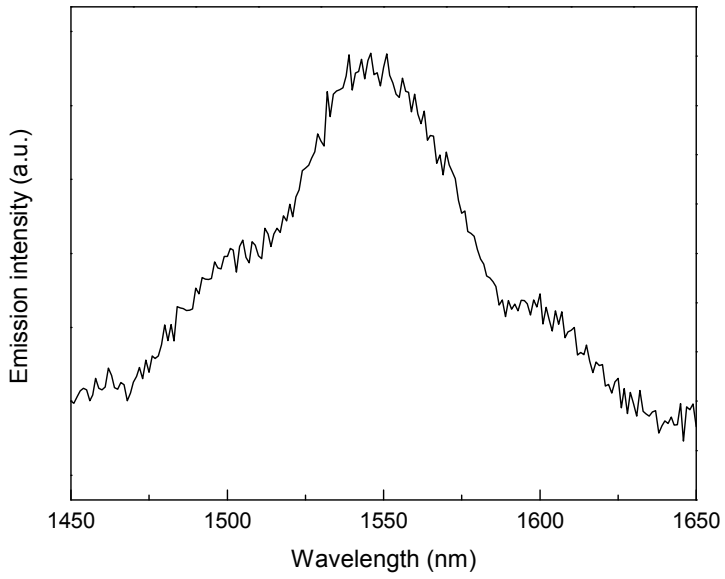

Fig. S63 Emission spectrum of $[P_{4444}]_3[ErCl_6]$, excited at 355.0 nm (uncorrected spectrum).

2) Excitation spectrum

Monitoring the emission of the sample at 1545.0 nm (6472 cm^{-1}, $^4I_{13/2} \rightarrow {}^4I_{15/2}$ transition), the excitation wavelength was varied between 250 and 700 nm to record an excitation spectrum (Fig. S64). Three peaks are visible in the spectrum and can be assigned to transitions within the Er^{3+} ion's 4f shell. The peaks labelled a-c have been assigned to the corresponding transitions in Table S31.

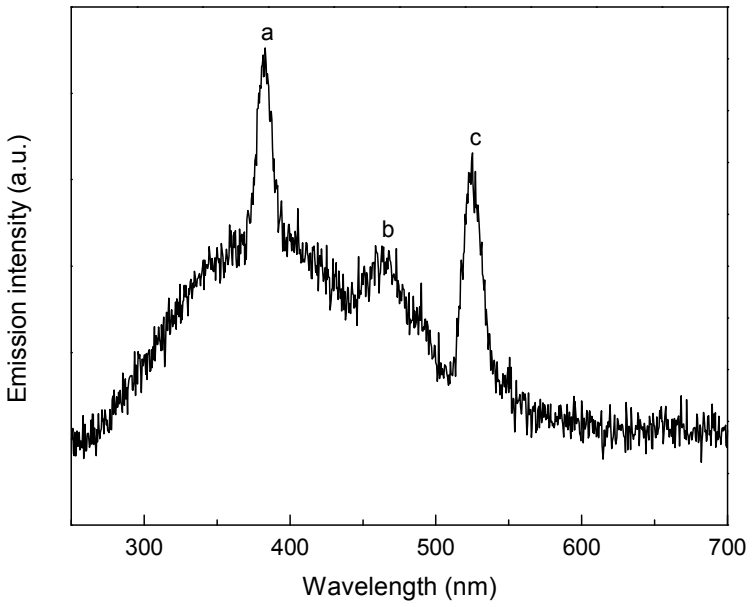

Fig. S64 Excitation spectrum of $[P_{4444}]_3[ErCl_6]$, monitored at 1545.0 nm (uncorrected spectrum).

Table S31. Assignment of the 4f-4f transitions in the excitation spectrum of $[P_{4444}]_3[ErCl_6]$.

Label	λ (nm)	$\bar{\upsilon}$ (cm^{-1})	Transition
a	383.0	26110	$^4G_{11/2}\leftarrow{}^4I_{15/2}$
b	464.0	21552	$^4F_{3/2}$, $^4F_{5/2}$, $^4F_{7/2}\leftarrow{}^4I_{15/2}$
c	525.0	19048	$^4H_{11/2}\leftarrow{}^4I_{15/2}$

3) Luminescence decay times of $[P_{4444}]_3[ErCl_6]$

Upon excitation at 355.0 nm with a pulsed light source, the emission at 1545.0 nm shows a mono-exponential decay profile. The luminescence decay profile is given in Fig. S65. The luminescence decay time is calculated as 2.066 μs or 2066 ns.

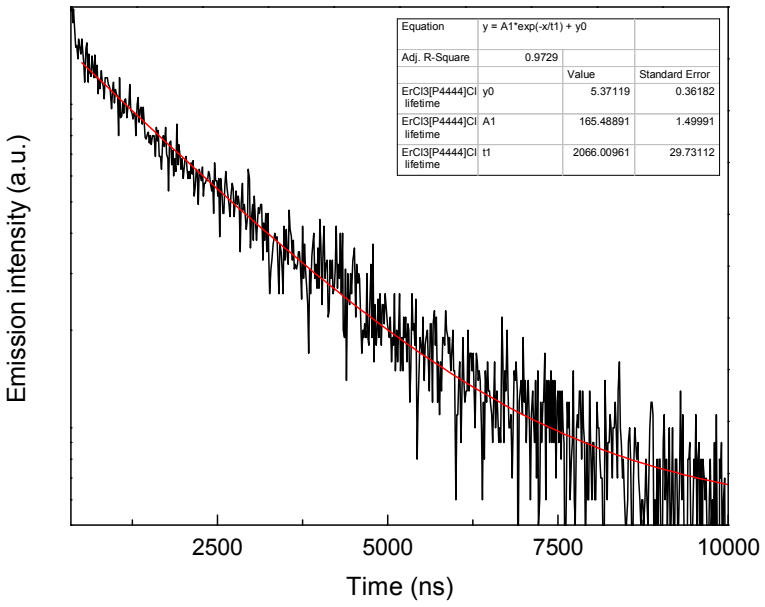

Fig. S65 Luminescence decay profile of $[P_{4444}]_3[ErCl_6]$ upon excitation at 355.0 nm and monitoring the emission decay at 1545.0 nm.

Luminescence properties of sample $[P_{4448}]_3[ErCl_6]$

1) Emission spectra

Upon excitation at 355.0 nm (28169 cm^{-1}), in the $^4G_{11/2} \leftarrow {}^4I_{15/2}$ transition, the sample shows only one narrow emission peak of Er^{3+} (Fig. S66). This peak, with a maximum at 1545.0 nm (6472 cm^{-1}), can be assigned to the $^4I_{13/2} \rightarrow {}^4I_{15/2}$ transition. As in the previous case the emission was very weak and 20 scans were needed to record the emission spectrum presented below.

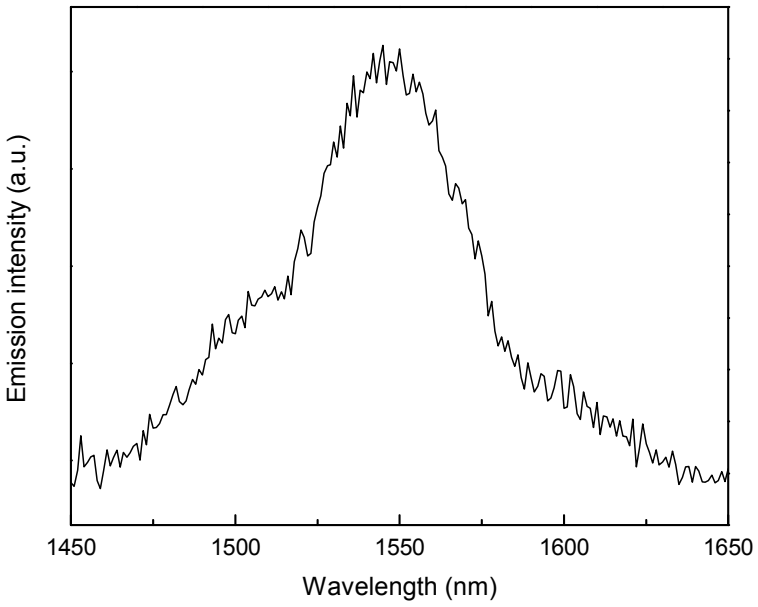

Fig. S66 Emission spectrum of $[P_{4448}]_3[ErCl_6]$, excited at 355.0 nm (uncorrected spectrum).

2) Excitation spectrum of $[P_{4448}]_3[ErCl_6]$

Monitoring the emission of the sample at 1545.0 nm (6472 cm^{-1}, $^4I_{13/2} \rightarrow {}^4I_{15/2}$ transition), the excitation wavelength was varied between 250 and 700 nm to record an excitation spectrum (Fig. S67). Four peaks are visible in the spectrum and can be assigned to transitions within the Er^{3+} ion's 4f shell. The peaks labelled a-d have been assigned to the corresponding transitions in Table S32.

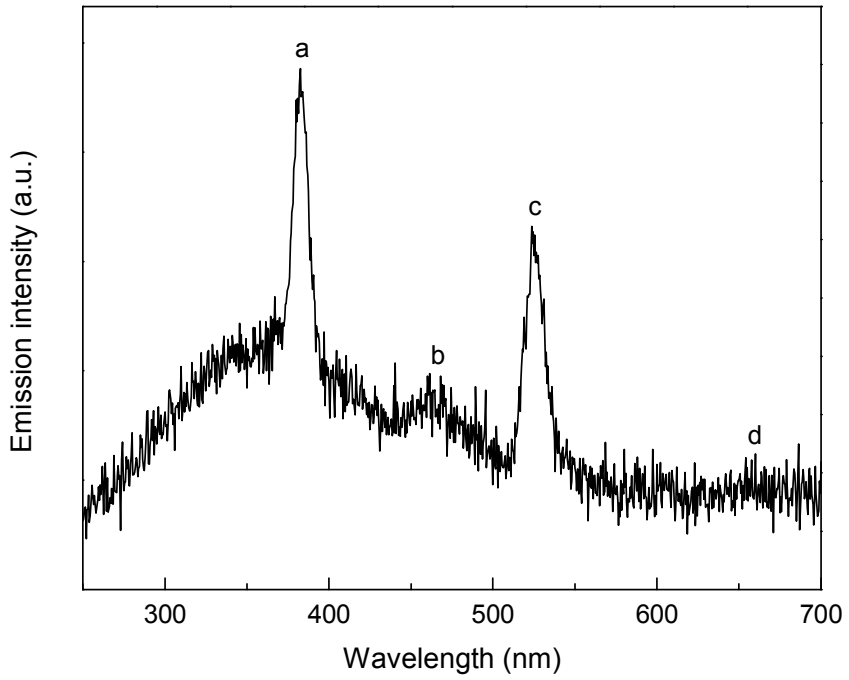

Fig. S67 Excitation spectrum of $[P_{4448}]_3[ErCl_6]$, monitored at 1545.0 nm (uncorrected spectrum).

Table S32. Assignment of the 4f-4f transitions in the excitation spectrum of $[P_{4448}]_3[ErCl_6]$.

Label	λ (nm)	$\bar{\upsilon}$ (cm^{-1})	Transition
a	382.0	26178	$^4G_{11/2} \leftarrow {}^4I_{15/2}$
b	468.0	21368	$^4F_{3/2}$, $^4F_{5/2}$, $^4F_{7/2} \leftarrow {}^4I_{15/2}$
c	523.0	19120	$^4H_{11/2} \leftarrow {}^4I_{15/2}$
d	660.0	15152	$^4F_{9/2} \leftarrow {}^4I_{15/2}$

3) Luminescence decay times of $[P_{4448}]_3[ErCl_6]$

Upon excitation at 355.0 nm with a pulsed light source, the emission at 1545.0 nm shows a mono-exponential decay profile. The luminescence decay profile is given in Fig. S68. The luminescence decay time is calculated as 2.736 μs or 2736 ns.

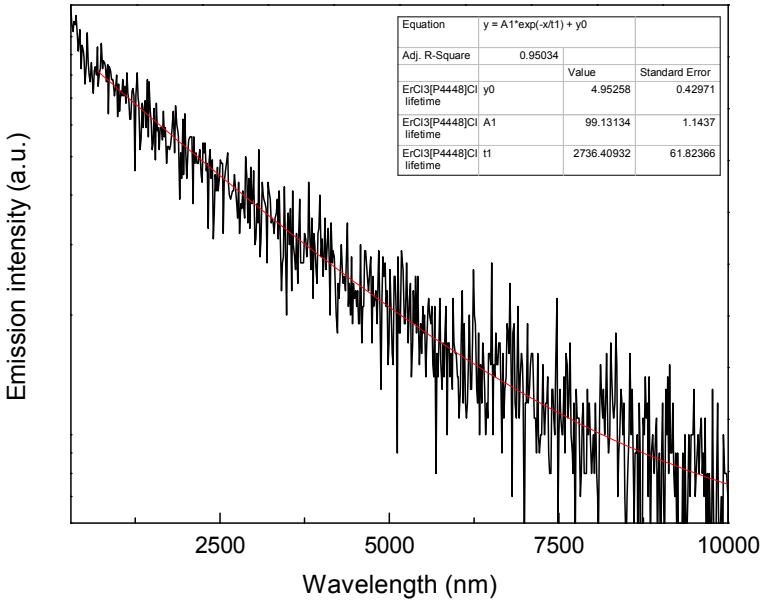

Fig. S68 Luminescence decay profile of $[P_{4448}]_3[ErCl_6]$ upon excitation at 355.0 nm and monitoring the emission decay at 1545.0 nm.

Luminescence properties of sample $[P_{666\ 14}]_3[ErCl_6]$

1) Emission spectra

Upon excitation at 375.0 nm (26667 cm^{-1}), in the $^4G_{11/2} \leftarrow {}^4I_{15/2}$ transition, the sample shows only one narrow emission peak of Er^{3+} (Fig. S69). This peak, with a maximum at 1543.0 nm (6481 cm^{-1}), can be assigned to the $^4I_{13/2} \rightarrow {}^4I_{15/2}$ transition.

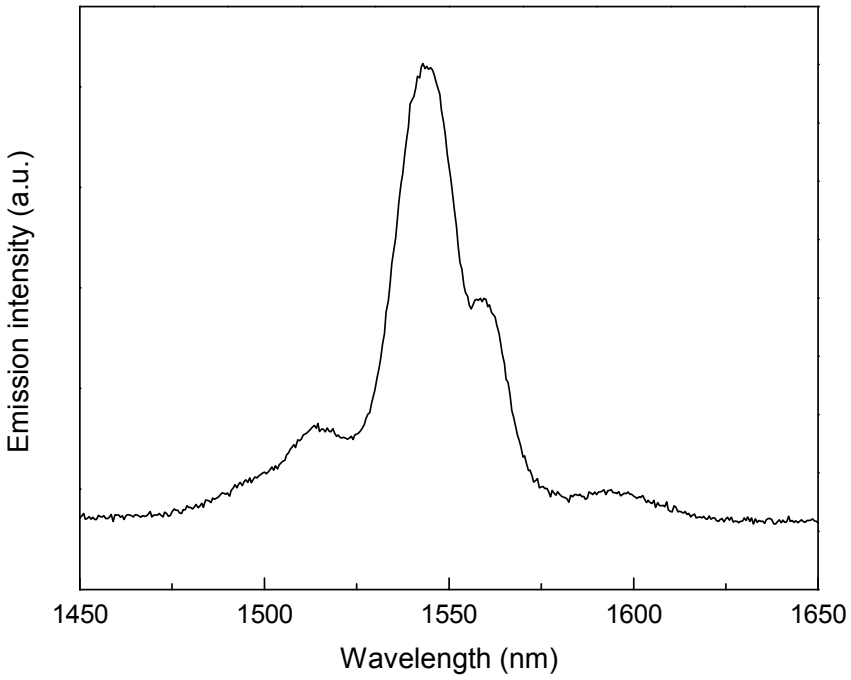

Fig. 69 Emission spectrum of $[P_{666\ 14}]_3[ErCl_6]$, excited at 375.0 nm (uncorrected spectrum).

2) Excitation spectrum of $[P_{666\ 14}]_3[ErCl_6]$

Monitoring the emission of the sample at 1543.0 nm (6481 cm^{-1}, $^4I_{13/2} \rightarrow {}^4I_{15/2}$ transition) the excitation wavelength was varied between 250 and 700 nm to record an excitation spectrum (Fig. S70). Three peaks are visible in the spectrum and can be assigned to transitions within the Er^{3+} ion's 4f shell. The peaks labelled a-d have been assigned to the corresponding transitions in Table S33.

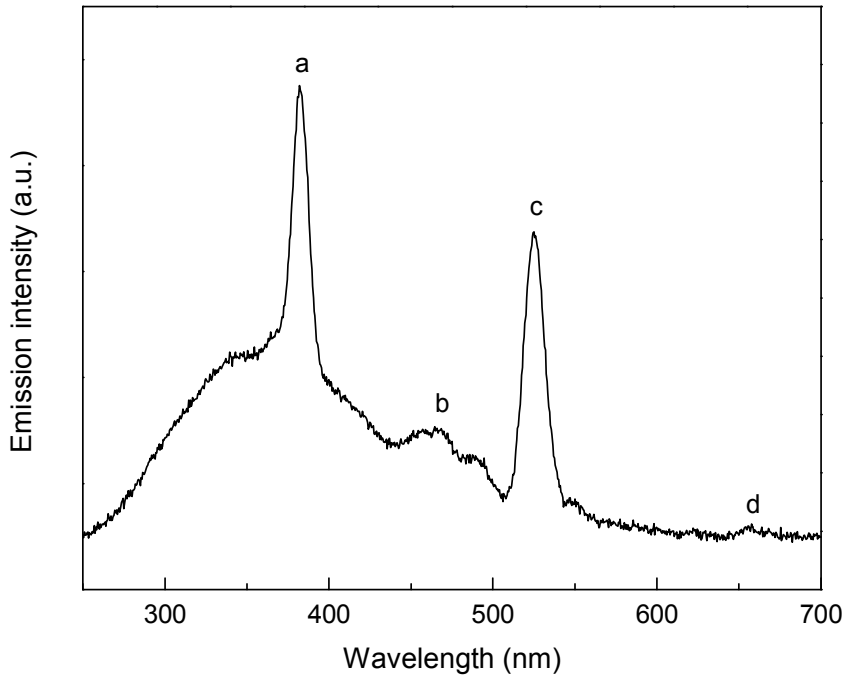

Fig. 70 Excitation spectrum of $[P_{666\,14}]_3[ErCl_6]$, monitored at 1543.0 nm (uncorrected spectrum).

Table S33. Assignment of the 4f-4f transitions in the excitation spectrum of $[P_{666\,14}]_3[ErCl_6]$.

Label	λ (nm)	$\bar{\upsilon}$ (cm^{-1})	Transition
a	382.0	26178	$^4G_{11/2} \leftarrow {}^4I_{15/2}$
b	465.0	21505	$^4F_{3/2}$, $^4F_{5/2}$, $^4F_{7/2} \leftarrow {}^4I_{15/2}$
c	525.0	19048	$^4H_{11/2} \leftarrow {}^4I_{15/2}$
d	655.0	15267	$^4F_{9/2} \leftarrow {}^4I_{15/2}$

3) Luminescence decay times of $[P_{666\,14}]_3[ErCl_6]$

Upon excitation at 355.0 nm with a pulsed light source, the emission at 1543.0 nm shows a mono-exponential decay profile. The luminescence decay profile is given in Fig. S71. The luminescence decay time is calculated as 2.725 μs or 2725 ns.

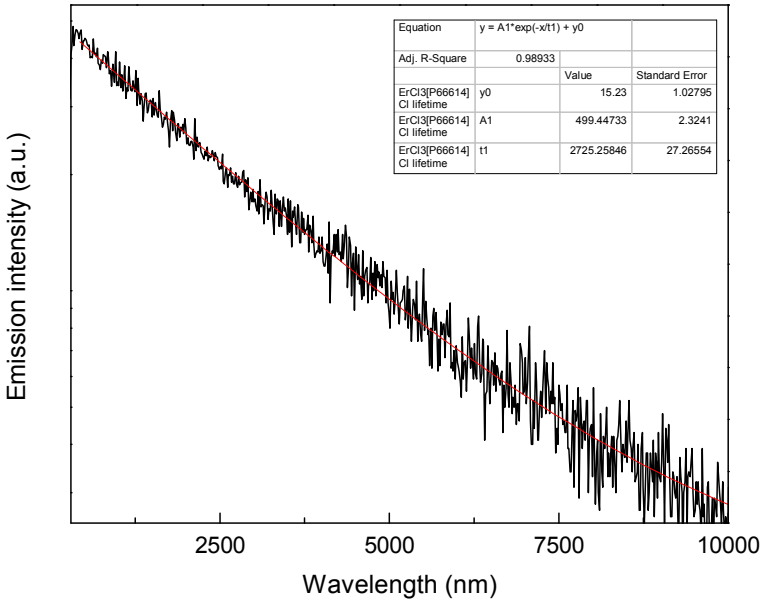

Fig. S71 Luminescence decay profile of $[P_{666\ 14}]_3[ErCl_6]$ upon excitation at 355.0 nm and monitoring the emission decay at 1543.0 nm.

Some excitation spectra and all near infrared emission spectra included in the report have not been corrected for the detector response. To explain this, we have included a corrected excitation spectrum of sample $[P_{4444}]_3[TbCl_6]$ to show the effect of such correction. In Fig. S72, the short wavelength part of the spectrum is blown out of proportion, because the detector has hardly any sensitivity at these wavelengths and as a result, overcompensates. The relative intensities of the transitions shown in this wavelength range would not have changed after correction and can therefore be trusted.

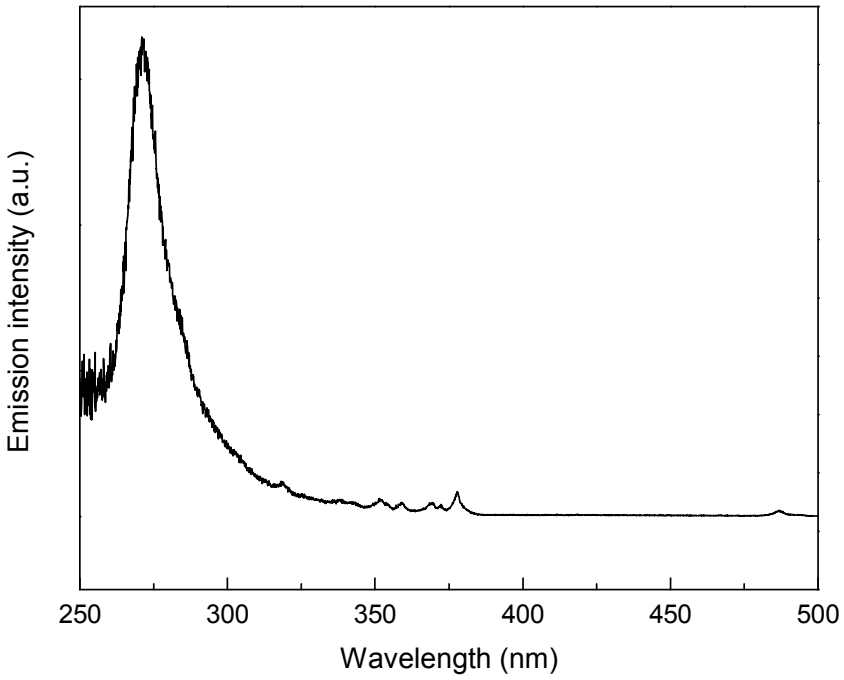

Fig. S72 Excitation spectrum of $TbCl_3[P_{4444}]Cl$, monitored at 546.2 nm and corrected for detector.

Table S34: CHN results for the $[P_{4444}]_3[RECl_6]$ series, $[P_{666\,14}]_3[RECl_6]$ (with RE = La, Ce, Pr, Nd, Sm, Eu, Gd, Tm, Tb, Dy, Ho, Er, Yb, Lu, Y, Sc) and the selected examples of the series $[P_{444\,8}]_3[RECl_6]$ (with RE = Ce, Pr, Nd, Sm, Eu, Gd, Tm, Tb, Dy, Ho, Er, Yb, Lu, Y, Sc).

RE metal	$[P_{4444}]^+$ / CHN (calc %; found %)	$[P_{4448}]^+$ / CHN (calc %; found %)	$[P_{666\,14}]^+$ / CHN (calc %; found %)
La	CHN(calc): C, 51.02; H, 9.63; CHN(found): C, 50.91; H, 9.58		CHN(calc): C, 63.94; H, 11.40; CHN(found): C, 63.60; H, 11.28
Ce	CHN(calc): C, 50.97; H, 9.62; CHN(found): C, 50.73; H, 9.53	CHN(calc): C, 55.46; H, 10.24; CHN(found): C, 55.54; H, 10.22	CHN(calc): C, 63.90; H, 11.40; CHN(found): C, 63.82; H, 11.27
Pr	CHN(calc): C, 50.93; H, 9.62; CHN(found): C, 50.78; H, 9.25		CHN(calc): C, 63.87; H, 11.39; CHN(found): C, 63.55; H, 11.40
Nd	CHN(calc): C, 50.78; H, 9.59; CHN(found): C, 50.60; H, 9.44	CHN(calc): C, 55.28; H, 10.21; CHN(found): C, 55.60; H, 10.01	CHN(calc): C, 63.76; H, 11.37; CHN(found): C, 63.51; H, 11.33
Sm	CHN(calc): C, 50.51; H, 9.54; CHN(found): C, 50.19; H, 9.43	CHN(calc): C, 55.02; H, 10.16; CHN(found): C, 55.60; H, 9.97	CHN(calc): C, 63.54; H, 11.33; CHN(found): C, 63.36; H, 11.31
Eu	CHN(calc): C, 50.44; H, 9.52; CHN(found): C, 50.33; H, 9.45	CHN(calc): C, 54.96; H, 10.15; CHN(found): C, 54.60; H, 10.04	CHN(calc): C, 63.48; H, 11.32; CHN(found): C, 63.19; H, 11.22
Gd	CHN(calc): C, 50.21; H, 9.48; CHN(found): C, 50.04; H, 9.47		CHN(calc): C, 63.30; H, 11.29; CHN(found): C, 63.33; H, 11.24
Tb	CHN(calc): C, 50.13; H, 9.47; CHN(found): C, 49.95; H, 9.39	CHN(calc): C, 54.67; H, 10.09; CHN(found): C, 54.47; H, 9.83	CHN(calc): C, 63.24; H, 11.28; CHN(found): C, 62.97; H, 11.15
Dy	CHN(calc): C, 49.98; H, 9.44; CHN(found): C, 49.81; H, 9.32	CHN(calc): C, 54.52; H, 10.07; CHN(found): C, 54.58; H, 10.28	CHN(calc): C, 63.12; H, 11.26; CHN(found): C, 62.88; H, 11.14
Ho	CHN(calc): C, 49.87; H, 9.42; CHN(found): C, 49.74; H, 9.42		CHN(calc): C, 63.03; H, 11.24; CHN(found): C, 62.79; H, 11.26
Er	CHN(calc): C, 49.77; H, 9.40; CHN(found): C, 49.69; H, 9.36	CHN(calc): C, 54.32; H, 10.03; CHN(found): C, 54.15; H, 9.79	CHN(calc): C, 62.95; H, 11.23; CHN(found): C, 62.83; H, 11.03
Tm	CHN(calc): C, 49.70; H, 9.38; CHN(found): C, 49.62; H, 9.29		CHN(calc): C, 62.90; H, 11.22; CHN(found): C, 62.91; H, 11.40
Yb	CHN(calc): C, 49.53; H, 9.35; CHN(found): C, 49.39; H, 9.25		CHN(calc): C, 62.76; H, 11.19; CHN(found): C, 62.84; H, 11.07
Lu	CHN(calc): C, 49.44; H, 9.34; CHN(found): C, 49.26; H, 9.29		CHN(calc): C, 62.69; H, 11.18; CHN(found): C, 62.50; H, 11.06
Y	CHN(calc): C, 53.39; H, 10.08; CHN(found): C, 53.27; H, 9.90		CHN(calc): C, 65.77; H, 11.73; CHN(found): C, 65.62; H, 11.69
Sc	CHN(calc): C, 55.65; H, 10.51; CHN(found): C, 55.58; H, 10.41		CHN(calc): C, 67.46; H, 12.03; CHN(found): C, 67.14; H, 11.93

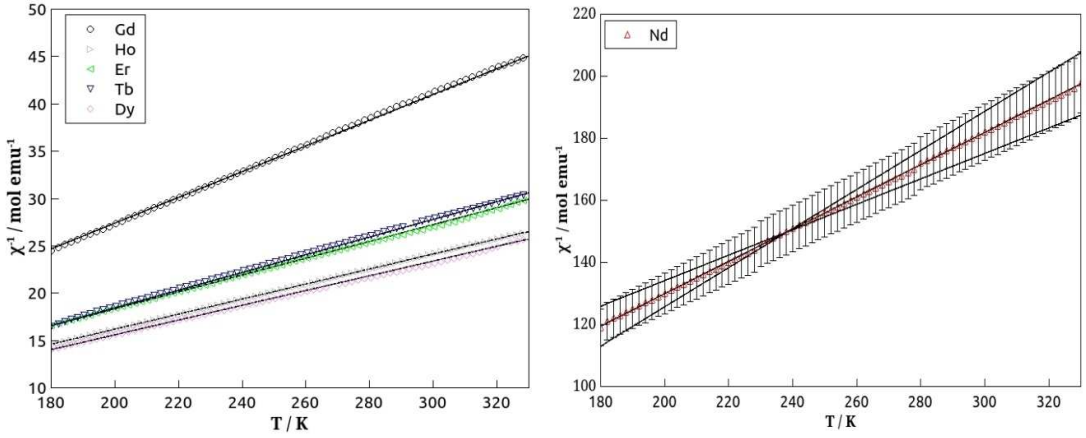

Figure S73. Magnetic susceptibility measurements for Er, Dy, Tb, Ho, Gd, (left) and Nd (right) samples in the temperature range 180K-330K, collected on heating with an applied field of 500Oe. The symbols represent the experimental data and the lines show the Curie-Weiss fits used to determine the effective magnetic moments. The Nd data shows error bars associated with the uncertainty in the measurement and the maximum and minimum lines of best fit.

Table S35. Curie constants and Weiss temperatures calculated from magnetic susceptibility for Er, Dy, Nd, Ho, Gd and Tb samples.

Lanthanide Ion	**Curie Constant, C, (emu K mol^{-1} Oe^{-1})**	**Weiss Temperature, θ (K)**
Dy	12.9±2.4	0±43.8
Nd	1.9±0.4	-49.5±63.8
Er	11.2±2.1	-6.2±44.7
Tb	10.7±1.8	2.7±38.6
Ho	12.6±2.4	-3.8±45.0
Gd	7.4±1.1	-1.5±42.8